ADAMA SCIENCE AND TECHNOLOGY UNIVERSITY

School of Mechanical, Chemical and Materials Engineering

Analysis on a composite B-pillar crashworthiness and occupant safety for side impact in sedan car

A Thesis Submitted in partial fulfillment of the requirements for the award of the degree of Master of Science in Automotive Engineering

By

Abeba Tsegay

Advisor: Mr. Mekonnen Liben (Asst. Professor)

MECHANICAL SYSTEMS AND VEHICLE ENGINEERING DEPARTMENT

January, 2019

Adama, Ethiopia

CANDIDATE'S DECLARATION

I hereby declare that the work which is being presented in the thesis entitled "***analysis on composite B-pillar crashworthiness and occupant safety for side impact in sedan car***" in partial fulfillment of the requirements for the award of the degree of Master of Science in Automotive Engineering is an authentic record of my own work carried out from February 2018 up to January 2018 under the supervision of Mr. Mekonnen Liben (Asst.Professor), Department of Mechanical and Vehicle Engineering, Adama Science and Technology University, Ethiopia.

The matter embodied in this thesis has not been submitted by me for the award of any other degree or diploma. All relevant resources of information used in this thesis have been duly acknowledged.

Abeba Tsegay	___________	___________
Candidate name	Signature	Date

This is to certify that the above statement made by the candidate is correct to the best of my knowledge and belief. This thesis has been submitted for examination with my approval.

Mekonnen Liben (Asst.professor)	_____________	____________
Advisor name	Signature	Date

ADAMA SCIENCE AND TECHNOLOGY UNIVERSITY

SCHOOL OF MECHANICAL, CHEMICAL AND MATERIALS ENGINEERING

MECHANICAL SYSTEMS AND VEHICLE ENGINEERING DEPARTMENT

Analysis on Composite B-Pillar Crashworthiness and Occupant Safety for Side Impact in Sedan Car

By

Abeba Tsegay

Approved by board of Examiners

______________________________	__________	__________
Chairman, Department graduate committee	Signature	Date
______________________________	__________	__________
Advisor	Signature	Date
______________________________	__________	__________
Internal Examiner	Signature	Date
______________________________	__________	__________
External Examiner	Signature	Date

ACKNOWLEDGMENT

This thesis would not have been possible without the continual input and guidance of my advisor Mr. Mekonnen Liben (Asst. Prof.), Adama Science and Technology University (ASTU); I would like to give my gratitude for his excellent suggestion, comments, continuous support and guidance throughout this research.

My great appreciations and gratitude also goes to Livermore University and Altire University for providing me licensed software's and all the support I needed. Without their help this thesis would have been difficult. I would love to give my thanks for MR. V.N. Ivan from Altire Forum for giving me all the support on the documents, tutorials and answers to all the questions I raised regarding the software's , it has been great experience.

I would also like to thank the Nyala and Awash Insurance Companies for providing me the information's they have.

TABLE OF CONTENTS

Contents **page**

LIST OF FIGURES

Figure **Page**

LIST OF TABLES

Tables **Page**

ACRONYMS

FEA	Finite Element Analysis
EuroNCAP	European New Cars Assessment Program
MDB	Moving Deformable Barrier
AEMDB	Advanced Euro Mobile Deformable Barrier
IIHS	Insurance Institute for Highway Safety
ECD	Easi Crash Dynamics
MADYMO	Mathematical Dynamic Models
LSDYNA	Liver more Dynamics software
TTI	Thoracic Trauma Index
HIC	Head Injury Criterion
Pa	Pelvic acceleration
Ha	Head acceleration
KE	Kinetic Energy
IE	Internal Energy
MPP	Massively Parallel processing machines

ABSTRACT

Drivers and passengers which involved in side impact collisions have high tendency to fatal injuries compared to frontal or rear impact collisions due to limited space in the passenger compartment. The passengers are subjected for different kinds of injuries; mainly brain injuries caused due to the intrusion of B-pillar inside the passenger cabin; through collision with the head of the occupant at the same time, due to different environmental conditions such as fuel consumption and emission, it is essential to decrease the structural weight of the vehicle. The objective was to analyze a composite B-pillar for minimum deformation and weight. This improves the vehicle crashworthiness and ensuring the safety of passenger during side crash accident. The B-pillar was designed following the standard methods and validated according to EuroNCAP and IIHS. In this thesis hyper mesh, hyper crash, MADYMO and LS DYNA were adopted for finite element analysis of a Ford Taurus B-pillar. To select the composite thickness and orientation, this study initially analyzes the B-pillar after being subjected to an even force of 140 KN. This resulted the selected B-pillar with thickness t = 4.15mm decrease in deformation up to 78.2 % and t=2.9mm up to 42.4% compared to the minimum B-pillar thickness t=1.6mm. The degree of orientation was set as 0°, 45°, 0°, 45°, 0°, 45°, 0°, 45°, and 0 °. The 1.1 kg composite B-pillar shows decrease in weight up to 57.9 % compared to 2.6 kg steel B-pillar. To ensure that EuroNCAP TP directives were met, both steel and composite pillars were merged with the vehicle and crashed into 254mm diameter rigid pole at a speed of 29 km/h. composite B-pillar showed 62.5 MJ energy absorbing capacity which increases by 50.4 % compared with steel B-pillar results 29.8 MJ. The composite and steel pillars resulted in a deformation of 399.4 mm and 579.1 mm respectively, which decrease in deformation up to 31.1 %. To ensure the occupant safety Hybrid III 50th percentile dummy were used. Composite B-pillar resulted in Head Injury Criterion (HIC) Thoracic Trauma Index (TTI) and pelvic acceleration of 263g's, 15g's and 75g's respectively that is 72.9 %, 62.5 % and 37.5 % less than steel pillar. This decreases the injury level of the passenger. This showed an improvement in the energy absorption and occupant safety and decrease in weight and deformation which can save passengers from injury and also fuel consumption.

Keywords: side impact, crashworthiness, B-pillar, steel, composite, hyper mesh, MADYMO, TTT,HIC

CHAPTER ONE

INTRODUCTION

1.1. Introduction about side impact

Vehicle accidents have become one of the major causes for increasing death rates of humans worldwide. Hence, stringent norms on vehicle safety have been imposed on automobile industries.

In various incidents, the accidents of the vehicles on the road the side impact have highest contribution to mortality. In a side impact, the occupants on both the struck, or near side, of the vehicle and the occupants on the opposite, or far side, of the vehicle are at risk of injury.

In side impact of a car, the impacting vehicle slows down due to the reaction force generated by different structural members like car doors, side impact beams, roof bow, B-Pillar etc. As these structural members plastically deform and absorb energy, the impacting vehicle decelerates. Of the many components, because of its size and location in the structure, B-Pillar has to absorb substantial energy with least amount of deformation in order to limit its intrusion in the passenger compartment [1]. Hence, it is very crucial in vehicle industry to confirm the crashworthiness of car, Crashworthiness is an engineering term used to define the ability of vehicle structure to absorb energy and protect its occupants during an impact [2].

As a result, some advanced methods have been developed to protect the occupants during side impact accidents. Tests and simulations similar to frontal impact safety tests are performed to evaluate a vehicle's side impact safety. Various side impact test methods exist, the moving deformable barrier (MDB) and pole side impact test are being used as the standard certified test on a car for side impact safety analysis [4].

Due to increasing legal and market demands for safety, the weight of a conventional car body will most likely increase in the future. At the same time, environmental demands will become stronger and lower weight will play an important part in meeting them. In the European Union, the car manufacturers have agreed to an overall 25% increase in fuel efficiency by the year 2005 compared to 1990 [5]. These demands contradict each other and there are essentially two means of satisfying them both,

- The use of new materials, with low weight but high strength and stiffness.
- Optimization of the structure, i.e. using the structure as efficiently as possible [5].

This thesis project deals with the first one. A Ford Taurus vehicle is selected which represents the sedan car. It is medium weight of 1625 kg and is used for side impact analysis by Euro NCAP test protocol as a test vehicle. In order to investigate the materials strength software's like Hyper Mesh, LS DYNA and MADYMO are used.

1.2. Background and justification

The significance of high strength and rigidity are fundamental prerequisite for any vehicle occupant's cell, this cannot be overemphasized due to the protection it provides against accident, particularly side impacts which greatly rely upon rigidity of what is referred to as safety cage [6]. Road safety report describes an occupant cell as a '*survival box'* and suggests that the survival of occupants involved in the circumstance of an accident depend highly on the strength of the cell which is a fundamental prerequisite for vehicle safety design Other factors such as bad design, wrong communication, wrong decision, risk taken etc. can equally lead to road accident. According to [6] causalities, communication, socioeconomic, and sociocultural issues are important to understand nature of risks and to make correct decisions. From this point of view, it imperative that the frame and other supporting parts of a vehicle be properly designed to ensure safety and prevent loss of life in the event of accidents. As shown in Figure 1.1, there are three main pillars supporting the frame work of a typical vehicle and these includes A-pillar, B-pillar and C-pillar, but some vehicles with very large compartment has additional pillar supporting structure at its rare side known as D pillar. Moreover, each of the aforementioned pillars found in a car plays a vital role in the performance of a car but the B-pillar is one of the most important vehicles supporting structure [6].

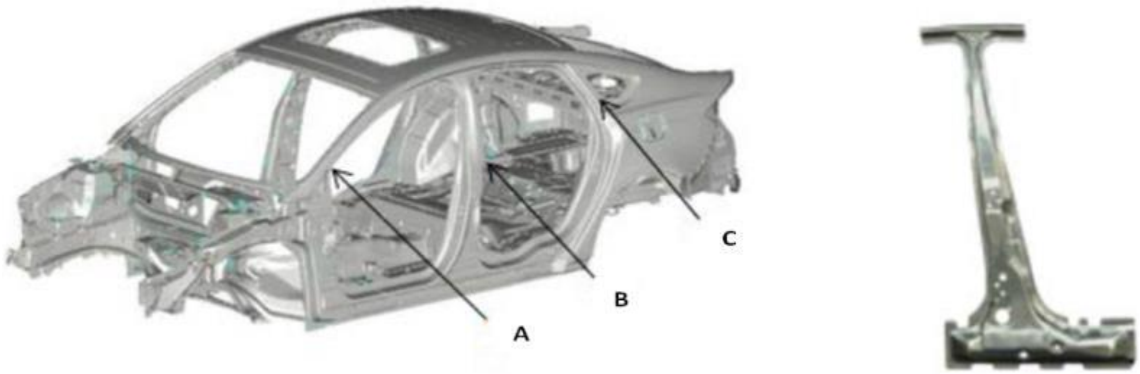

Figure 1.1. Typical supporting pillars and their locations in a vehicle

The B-pillar also known as a “post” serves as a supporting member to a car’s roof panel and it is also mounted sideward at the mid-section of a car for latching the front door and installation of the inches for the rare door. For installation purpose, B-pillar is a vertically closed steel structure welded to the vehicle’s rocker panel and floor pan at the base and to the roof panel at the top. This project focuses mainly on the B-pillar strength when exposed to external force side impacts caused by accidents or events that may affect the geometry of the car and occupants safety when using lightweight materials. As probably one of the most complex structural member that supports and maintains the geometry of a vehicle’s roof, the B-pillar manufacturing may involve multi-layered assembly of various material strength and length. B-pillar is a very essential part of a car, and the stability of the occupant cell depends highly on the strength and rigidity of the pillar hence, necessitating proper design of the B-pillar for safety purpose against side collision or impact [6].

Accident investigation by Carney [6] revealed that 1 out of 5 accident results in side impact which accounts for 75% of vehicle occupant injury. Hence, for protection of passengers in accidental scenarios, the B-pillar design and manufacturing must be in line with existing standards and techniques to enhance resistance to impact which may depend on a number of factors including material and welding techniques. Therefore, in order to validate the efficiency of a B-pillar for proper design and material selection it is necessary for the design to be analyzed by Finite Element Analysis and modeled using appropriate Computer Aided Engineering software’s. FEA is a numerically analysis techniques for structural engineering designs. This involves design with the aid of complex software and FEA solvers, which can be used in analyzing the effect impacts, vibration stress, heat transfer etc. [6].

Many researchers have done various studies on frontal and side impact crash analysis and have been successful in reducing the death rates and injury risks that affect the passengers. From figure 1.2 it can be seen that over the past two decades the researches on frontal impact has helped in reducing injuries, however, the injuries due to side impact crash has increased [3].

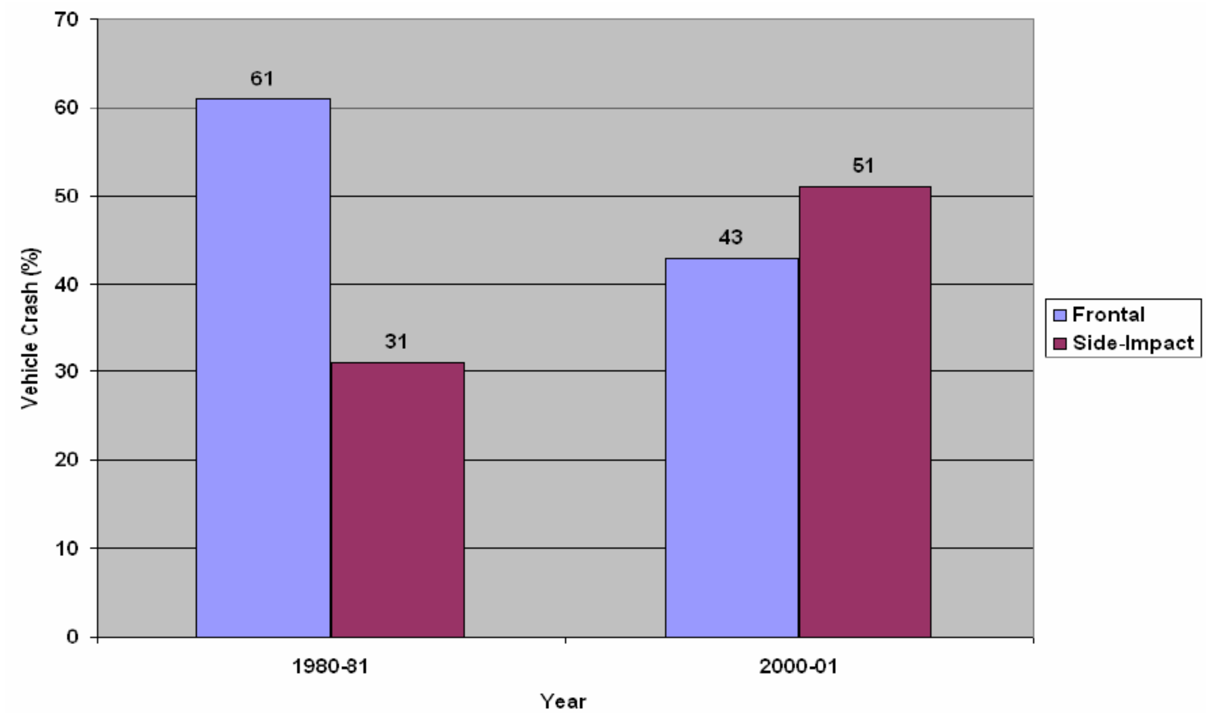

Figure 1.2. Comparison of frontal and side impact crash

According to studies done in Ethiopia [7] the quantity of police – reported traffic crashes in Ethiopia in six years (July 2005 – June 2011) consists of 12,140 fatal and 29, 454 injury crashes on the country's road network due to different types of crashes. The crashes by side collusion type were 260 fatal crashes and 262.14 injury crashes out of total 522.14 side crashed. This indicates the fetal rate is 50 % out of the total side crashes. The crashes by automotive vehicle type were 1204 fatal and 5606 injury crashes [7]. NHTSA found that in side impacts face and head injuries accounted for 40% of fatalities and 13% of injuries [26].

1.3. Statement of the problem

Various studies have indicated that Ethiopia has one of the highest rates of fatality per vehicle in the world. Side crash is leading cause of mortality due to the close proximity of occupant to the collision point comparing to frontal crash. These occupants are subjected for different kinds of injuries; mainly brain injuries caused due to the intrusion of B-pillar inside the passenger cabin; through collision with the head of the occupant. NHTSA found that in side impacts face and head injuries accounted for 40% of fatalities and 13% of injuries. In Ethiopia from the total side crash that occurs 50% are fetal as a result extent of B-Pillar intrusion determines occupant injury levels and hence, structural rating.

In another case due to different environmental conditions such as fuel consumption and emission, it is essential to decrease the structural weight of the vehicle.

So in order to meet both automotive engineering aspects there is a need to advance the B-pillar structure crashworthiness and reduction in vehicle weight.

1.4. Objective

1.4.1. General objective

The general objective of this thesis is to analyze the crashworthiness of composite B-pillar for occupant safety in case of side impact crashes on sedan car.

1.4.2. Specific objectives

The specific objectives are as follows:-

- To study and analyze the deformation rate and energy absorbing capacity of exiting steel B-pillar.
- To analyze the deformation rate and energy absorbing capacity of composite B-pillar.
- To analyze the injury criteria of an occupant.
- To validate the results according to Euro NCAP test protocol rules, experimental results and IIHS rules and regulations.

1.5. Significance of the study

Vehicle crash is becoming the second most cause of death. Ethiopia has one of Africa's fastest growing non-oil producing economies and an increasing level of motorization. This rapidly increasing mobility has created some unique road safety concerns. Vehicle side crash is increasing every year due to different reasons. Some of the reasons are vehicle structural strength, driver mistakes, road environment and soon. This study has a great contribution in decreasing the fetal caused due to structural strength of the vehicle. As a result this study has the following significances;

- Improving the crashworthiness of the car in side impacts.
- It helps in reducing the injuries and fatality rate.
- It is helpful in reducing the weight of the vehicle.
- It also helps in reduction of pollution due to reduction in the weight.
- This work will be beneficiary to the automobile industries, vehicle owners, society and the country as whole, future researchers also get benefited.

1.6. Scope of the study

In this project the Finite Element model of Ford Taurus is used. Several laboratory tests, simulations, Euro NCAP Test Protocol and IIHS (Insurance Institute for Highway Safety) are required for validation of the FE model for simulation based approval.

- The composite stress, strain and deformation are analyzed to select the material thickness and orientation using optistruct solver.
- B-pillar of Ford Taurus will be studied using steel, and analyzed for energy absorption and deformation using Hyper Mesh.
- After analyzing the energy absorbing capacity of steel then the B-pillar is modeled using composite material, it is then analyzed for energy absorption and deformation using Hyper Mesh.

- Investigate if the composite material has a better energy absorbing capacity and less intrusion when compared to steel and are validated using experimental tests and simulations from Euro NCAP Test Protocol.
- The occupant safety is analyzed using MADYMO and LS DYNA and is validated according to IIHS.

1.7. Limitations

The results of the study clearly showed that with the considered cases of operating scenarios, the vehicle B-pillar structure is improved. But limitations of the study are:

- Strength analysis of the pillar
- Experimental tests of the pillar property
- Experimental crash test of the pillar of the vehicle

1.8. Organization of the study

The study will be organized into five chapters. It starts with the introduction, which includes background, statement of the problem, objectives, scope and limitation of the study as well as the significance of the study. The second chapter will be review of literatures that deals with concepts and past studies and information pertinent to the study. The third chapter will explain research methodology including materials used and methods to be followed to accomplish the thesis work. In the fourth chapter result verification and discussion and in the last chapter conclusion and recommendation will be carried out.

CHAPTER TWO

LITERATURE REVIEW

2.1. Crashworthiness and Occupant Safety

Crashworthiness is the study of mechanical behavior of automotive structures in the advent of a crash. To have better crashworthiness performance, all the major structural components are required to participate efficiently and effectively in absorbing the crash-induced energy. The structural energy absorption directly affects the safety of vehicle occupants by substantially reducing the acceleration felt by the occupants as well as the possibility of the deformed structure coming in contact with the occupants, both of which could cause significant injury [8].

2.2. Features of B-Pillar

B-pillar is made up of various symmetrical or structural components. Although the pillar design varies depending on the manufacturers, for interest of occupant protection in event of lateral impact or accident in the side direction, it is important to note that a vehicle structure still consist of other component which form part of the protection structure and these includes C-pillar, A-pillar, Rocker panel, Floor pan, Roof panel etc. as illustrated in Figure 2.1. As mentioned earlier, one major advantage of the B-pillar is the provision of high level protection for passengers as well as the driver in cases involving intense side impact.

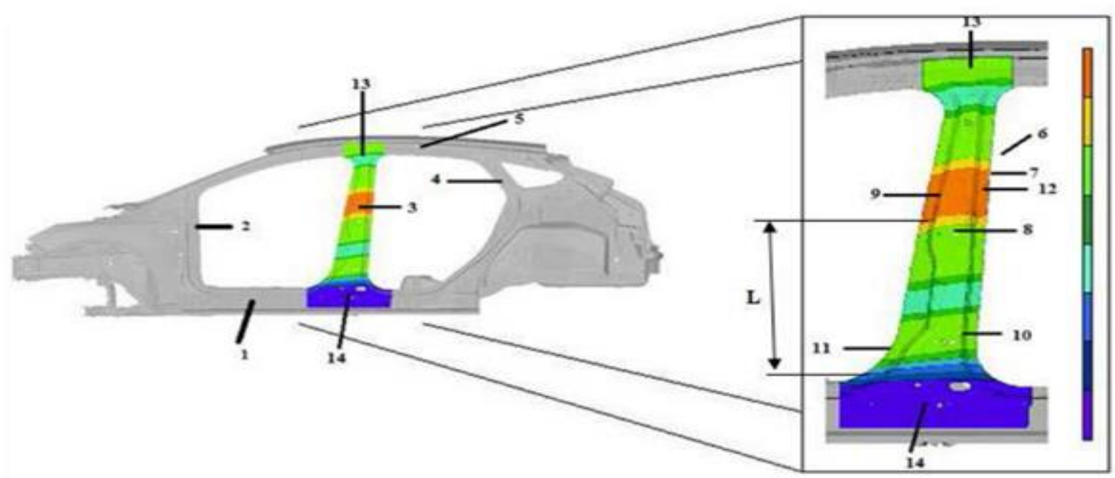

Figure 2.1. Fundamental features of a B-pillar

Figure 2.1 depicts the fundamental features of the B-pillar with regards to its position in the framework of direction of a vehicle structure, and side view. It also shows the connection or mating of the B-pillar with various other structural members to form a full lateral direction of an occupant cell. The A, B and C Pillars are designated as (2), (3) and (4), and are attached together by the process of welding to the floor pan labeled as (1). Also, the roof rail or panel labeled as (5) is welded to the uppermost end of the B-pillar. Furthermore, other parts of the B-pillar labeled 6, this consist of a curved-like member labeled as (7), while the center flange is labeled (8), the two web-like segments labeled (9) and 10 and both side flanges designated as (11) and (12). The lower and upper end section labeled (13) and (14) are the segments connecting the floor pan and the roof rail. Moreover, the length (L) signifies the softer area of lateral flanges (11) and (12) of the B-pillar. It is about 50% of the entire length of the flanges on the side [6]. Moreover it is indicated by shady part around the side flange which is the soft zone as well a variable depending on the requirement such as cover plate design and deformation properties. In crash cases involving side impact for example, the mid-section upper and base of the B-pillar are mostly affected, but good stiffness, fracture toughness and yield strength will minimize the chances of catastrophic failure under high loading impact. This is where the dissipation of impact energy is absorbed in form of plastic deformation which in turn improves the safety of the occupants of the vehicle. The aforementioned attributes describe the important functions and characteristics of a B-pillar. As mentioned earlier, the primary aim of a B-pillar is for occupant protection by minimizing the accident effect or side impact damage, particularly when the direction of impact is sideward [6].

2.3. Materials for B-pillar

Steel, the material typically used in vehicle structures, allowed for the economic mass production of millions of units over the past seven decades. Basic requirements for body structure materials include good formability, corrosion resistance, and recyclability. Body materials should also possess sufficient strength and controlled deformations under load to absorb crash energy, yet maintain sufficient survivable space for adequate occupant protection should a crash occur. Further, the structure should be lightweight to reduce fuel consumption. The majority of mass-produced vehicle bodies over the last six decades were manufactured from stamped steel components. Manufacturers build only a few limited production and specialty vehicle bodies from composite materials or aluminum. Although a patent for an all-steel body was granted in 1900, until the 1920's, automakers built vehicle bodies from a composite of wood panels joined with steel brackets. Steel sheets were added over the panels to provide a better surface to hold the paint. As metallurgists improved the formability of sheet steel and toolmakers built durable dies capable of stamping millions of parts and spot weld technology allowed for joining large body shells, the all-steel vehicle body became a reality. Dodge built an all-steel vehicle body in 1924 [9].

Steel

Steel sheets have been used in vehicle structures for more than one century. Its low production costs, consistent properties and the huge accumulated and available knowledge about its production processes make it the material of choice for automobile manufacturers. Its crashworthiness performance has been studied by several researchers [2].

Composite Materials

Composite materials have been investigated for their probable use as impact energy absorbing elements. Some of the composites that have been investigated for use in crashworthiness are random chopped fiber reinforced composites [2].

2.4. Energy absorbing capacity

Energy Absorbed Per Unit Mass

The energy absorbed per unit mass, or specific energy absorption, E, is defined as the energy absorbed by crushing E, per unit mass of deformed structure. This can be written as [8]:

$$E_S = \frac{E}{\rho \delta A_{mat}} = \frac{\int_0^\delta F dx}{\rho \delta A_{mat}} \quad (1)$$

For the ease of analysis, Eq. 1 is often estimated using an average collapse load, F or an average collapse stress σ. This approximate E s, given in Eq. 2 is sometimes known as specific sustained crushing stress.

$$E_s = \frac{F}{\rho A_{mat}} = \frac{\sigma}{\rho} \quad (2)$$

Specific energy absorption is an especially useful measure for comparing the energy absorption capabilities of different materials for structures in which weight is an important consideration.

Energy Absorbed Per Unit Volume

The energy absorbed per unit volume will be of interest in situations in which the space available for energy absorption deformation zone or device is in some way restricted [8]. It may also be appropriate when mechanisms other than deformation of the parent material contribute significantly to a structure's overall energy absorption capability.

Energy Absorbed Per Unit Length

The energy absorbed per unit length, L E from Eq.3 is defined as the energy absorbed per unit of deformation distance. This can be expressed as;

$$E_L = \frac{E}{\delta} \quad (3)$$

The energy absorbed per unit length provides a convenient and easily measured way of quantifying the crashworthiness of structures where collapse is restricted to a well-defined crumple zone [8]. A relatively straightforward crashworthiness specification such as this allows for the ready verification of structures with appropriate test procedures or finite element simulation. It can therefore be seen that the choice of the most suitable normalized energy absorption parameter for a given circumstance will depend upon the material and geometry of the crushed structure, as well as particular application under consideration.

2.4.1. Energy Absorption Capability of Composites for automotive application

The energy absorption capability [8], [9], [10] of the composite structure mainly depends on the

- Fiber Material – Physical properties of the fiber material directly influences the specific energy absorption of the composite. The brittle nature of the fiber results in more energy absorption rather than the ductile nature of the fiber, which fails by progressive folding.
- Matrix Material – Specific energy absorption linearly increases with the matrix compressive strength.
- Fiber and Matrix Combination – Due to crushing by high energy fragmentation, matrix material with a higher failure strain has high energy absorption than the fiber material.

- Fiber Orientation and Lay-up – High energy absorption composites consist of layers of specified orientation and sequence plies.

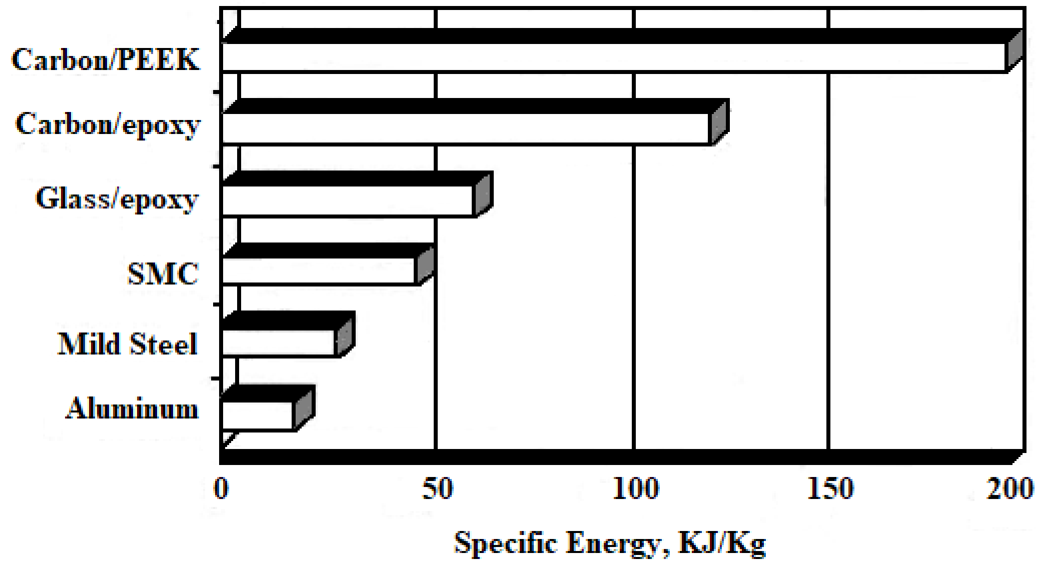

Figure 2.2. Specific energy of different materials

The composite materials have high specific energy absorption when compared to steel, as shown in the Figure 2.2. The properties like high specific strength and high specific stiffness are [10] attractive for the construction of lightweight and fuel efficient vehicle structures. The energy absorption capability of the composite materials offers a unique combination of reduced weight and improves crashworthiness of the vehicle structures [9], [10].

Fuel efficiency of the vehicle directly depends on the weight of the vehicle. The carbon fiber composite body structure is 57% lighter than steel structure of the same size and providing the superior crash protection, improved stiffness and favorable thermal and acoustic properties [10].

The composite materials are replacing most of the steel structures. Rotors manufactured using RTM (Resin Transfer Molding) for air compressor or super chargers of cars are used to substitute for metal rotors which are hard to manufacture [8].

The composite material was for the first time introduced to the formula-1 in 1980 by McLaren team. Since then the crashworthiness of the racing cars has improved beyond all recognition. They used the carbon fiber composite to manufacture the body, which is low weight, high rigidity and provided the high crash safety standards [10].

The light weight composite materials are already finding the exciting break in the automotive field as a means to increase the fuel efficiency. The vehicle weight directly contributes about 75 percent of fuel consumption. The vehicle industry can anticipate an aggressive 6 to 8 percent reduction in fuel consumption with 10 percent decrease in vehicle weight. This reduces around 20 kilogram of carbon dioxide emission per kilogram reduction in weight over the vehicle's lifetime [11].

The report from the United States and Canada predicted that plastics and composites would be widely used ap9plied to body panels, bumper systems, flexible components, trims, [11] drive shaft and transport parts of cars. Also rotors manufactured using RTM (Resin Transfer Moldings) for air compressor or superchargers of cars have been used to substitute for metal rotors which are difficult to machine [8].

2.4.2. MAT/LAW15 - Composite Shell Material

Description

This law is used to model composite shell elements, similar to law 25. The plastic behavior is based on the Tsai-Wu criteria (/MAT/LAW25 (COMPSH) for Tsai-Wu description) and failure is based on the Chang-Chang failure criterion is used. The effect of damage is taken in to account by decreasing stress components using a relaxation method to avoid numerical instabilities. Six material parameters are used in the failure criteria Where 1 is the fiber direction. The failure **criterion for fiber breakage is written as:**

Tensile fiber mode: $\sigma_{11} > 0$

$$e_f{}^2 = \left(\frac{\sigma_{11}}{S_1}\right) + \beta\left(\frac{\sigma_{11}}{S_1}\right)^2 - 1.0 \quad \geq 0\ failed \quad < 0\ elastic - plastic \tag{4}$$

Compressive fiber mode: $\sigma_{11} < 0$

$$e_c{}^2 = \left(\frac{\sigma_{11}}{c_1}\right)^2 - 1.0 \quad \geq 0\ failed \quad < 0\ elastic - plastic \tag{5}$$

For matrix cracking, the failure criterion is:

Tensile matrix mode: $\sigma_{22} > 0$

$$e_m{}^2 = \left(\frac{\sigma_{22}}{S_2}\right)^2 + \beta\left(\frac{\sigma_{12}}{S_{12}}\right)^2 - 1.0 \quad \geq 0\, failed \quad < 0\, elastic - plastic \qquad (6)$$

Compressive matrix mode: $\sigma_{22} < 0$

$$e_d{}^2 = \left(\frac{\sigma_{22}}{2S_{12}}\right)^2 + \left[\left(\frac{c_2}{2S_{12}}\right)^2 - 1\right]\frac{\sigma_{22}}{c_2} + \left(\frac{\sigma_{12}}{S_{12}}\right)^2 - 1.0 \quad \geq 0\, failed \quad < 0\, elastic - plastic \qquad (7)$$

2.5. Vehicle side impact crashworthiness tests

Side impacts are the most common and regularly result in extremely dangerous crashes and these are classified as vehicle to vehicle and vehicle to narrow object (pole, tree, etc) impact [12]. Tests and simulations similar to frontal impact safety tests are performed to evaluate a vehicle's side impact safety. Various side impact test methods exist, the moving deformable barrier (MDB) and with pole side impact test are being used as the standard certified test on a car for side impact safety analysis [4].

2.5.1. Pole side impact

The pole side impact test, according to EuroNCAP pole side impact test protocol as shown in Figure 2.3, was performed in the Automobile Crash Laboratory of Tsinghua University, Beijing. The test vehicle was placed on a large planar trolley, which allowed the free motion of the vehicle to be no less than 1 m. The trolley and the vehicle were accelerated together to 29 km/h, impacting a 254-mmdiameter rigid cylinder pole. The impact position aimed at the center of the gravity (C.G.) for the dummy head. Since the test vehicle was not equipped with a side airbag system, no dummies were used in this pole side impact test. However, the impact position was decided by the ES-2 dummy sitting in the driver seat. At the same time, finite element simulation of the same impact situation was conducted and the model was validated against the test results. The simulated results were compared with test data in terms of time histories of acceleration measured at the "low" point of the B-pillar on the unstruck side, the velocity derived from the acceleration, and the side permanent deformations [4].

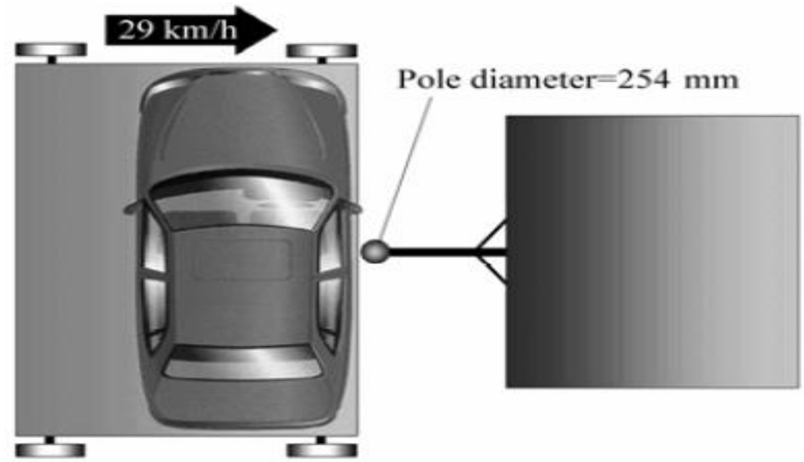

Figure 2.3. Pole side impact test

2.5.2. Moving deformable barriers (MDB) Standards for Side Impact Vehicles

The analysis usually carried out for side impact on a vehicle before the parts are assembled is an example of a real life situation of accident scenario. This is carried out to determine the amount of force required to damage the B-pillar in such a manner that may severely affect the passenger sitting by the side. During the test procedures, if the B-pillar absorbs a certain amount of force without any serious damage to the car, such B-pillar can be considered suitable to protect passengers in incidents that involves serious side impact, but if the impact test proves otherwise, then more reinforcement has to be carried out before the vehicle parts are assembled. The impact test description is illustrated as shown in Figure 2.4.

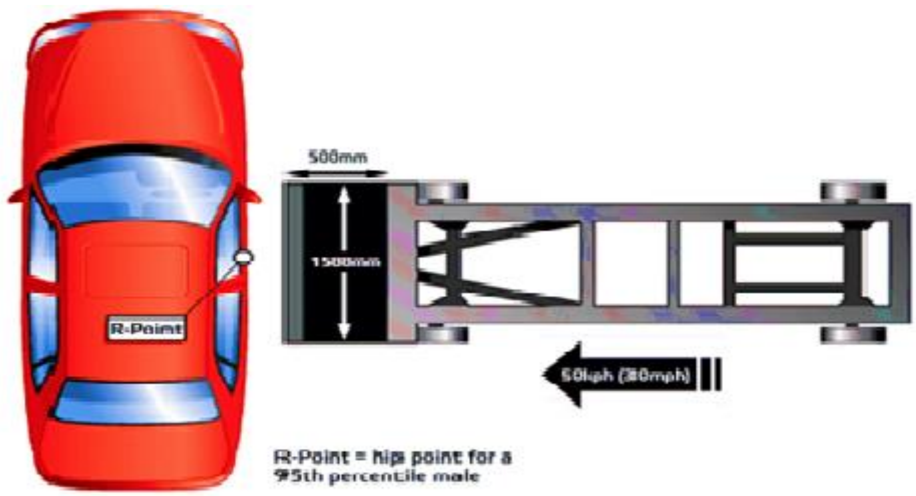

Figure 2.4. Moving deformable barriers (MDB) impact test

The impact test involves 500 X 1500mm impact requirements for the side collision on the driver of a fixed car at a speed of 50km/h as shown in Figure 6, and this requirement in recent times has been improved of which now goes by the name Advanced Euro Mobile Deformable Barrier (AEMDB). The changes in dimension include 500± 2.5x1700±2.5mm in comparison to the other dimensions shown in Figure above. The Current Side impact test requirements for AE-MDB is listed as follows

- The static displacement of car must be 340± 20mm.
- The total speed of must be 50km/h.
- The dynamic peak displacement must be 346± 20mm.
- The total weight must be 1300± 20kg.
- The movable barrier total energy absorption must be 61±5kJ.

Moreover, there are rules guiding the minimum standard requirement of new vehicles although to increase the safety standard of a vehicle or to ensure that the minimum requirement by law are met by vehicle manufacturing companies, numerous international organization responsible for monitoring and developing standard procedures for the impact test have evolved over the years to evaluate the safety of vehicles in the automotive industry.

It is imperative that side impact standards be considered as a guideline for FEA of a B-pillar, as this can provide details to the designer as to the amount of force that can affect the B-pillar performance, by so doing, the designer may consider reinforcing the B-pillar with suitable materials, and techniques. Euro NCAP standard evaluation of side impact suggests two methods namely; pole side impact and Car to Car side impact. The car to car side impact is illustrated in Figure 6, where a simulation crash is carried out by a movable deformable barrier [4].

2.6. Computer Aided Engineering Tools

Due to increasing cost on conducting real-time crash simulations, CAE tools are very widely used in auto industry. As a result, automakers have reduced product development cost and time while improving safety, comfort, and durability of the vehicles they produce. The predictive capability of CAE tools has progressed to the point where much of the design verification is now done using computer simulations rather than physical prototype testing. Tools used in this study are briefly explained below.

2.6.1. LS-DYNA

LS-DYNA is a general purpose transient dynamic finite element program capable of simulating complex real world problems. It is optimized for shared and distributed memory UNIX, Linux, and Windows based, platforms. It is an explicit 3-D finite element program for analyzing the large deformation dynamic response of the elastic and inelastic solids and structures. The program is extensively used by many top automobile, aerospace and research organizations. A wide range of material types and interfaces enable the efficient mathematical modeling of many engineering problems [20].

It contains more than one hundred and fifty material models including metallic, non-metallic and composite models which enable to define any material in the real world. The contact capabilities such as contact between deformable bodies, between deformable and rigid bodies provided in LS-DYNA can solve any contact problems which very useful in crash testing.

The main application areas of LS-DYNA are as follows:

- Crashworthiness simulations: automobiles, airplanes, trains, ships, etc.
- Occupant safety analyses: LS-DYNA integrated with MADYMO is used for dummy interaction with airbag, seat belts, foam padding, etc.
- To simulate Bird strike to airplanes.
- Analysis and optimization of Metal forming process.
- Biomedical applications and many more.

LS-DYNA computes on leading UNIX machines, supercomputers mad Massively Parallel Processing (MPP) machines. Computer configuration depends on processing time and problem size. Super computers and MPP takes the advantage of multiple processes when the code is highly efficient [20].

2.6.2. Easi Crash Dynamics (ECD)

EASI CRASH DYNA is the first fully integrated simulation environment specially designed for crash engineering requiring large manipulation capability. It can directly read files in IGES, NASTRAN, PAM-CRASH, MADYMO and LSDYNA data. ECD has unique features, which enable the crash simulation more realistic and more accurate.

Pre-Processing Features [20]

- Fully automatic meshing and automatic weld creation
- Rapid graphical assembly of system models
- FE-Dummy and Rigid body dummy structuring, positioning and orientation
- Material database access and manipulation
- Graphical creation, modification and deletion of contacts, materials, constraints and I/O controls
- Automatic detection and correction of initial penetration
- Replacing the component from one model to another model

Post-Processing Features [20]

- Highly optimized loading and animation of DYNA results for design
- Superposition of results for design

- User friendly and complete plotting for processing simulation and test data comparisons
- Quick access to stress energies and displacements without reloading the file
- Dynamic inclusion/exclusion of parts during animation and visualization
- Import and super-imposition of test results with simulation results
- Synchronization between animation and plots, between simulation result file and test result file

EASI-Plot Features [20]

- User friendly complete plotting tool for processing simulation and test data
- Easy access to engineering functions
- Plot file re-generation using template and session file

2.6.3. MADYMO

MADYMO (Mathematical Dynamical Models) is a general-purpose software package, which can be used to simulate the dynamic behavior of mechanical systems [13]. Although originally developed for studying passive safety, MADYMO is now increasingly used for active safety and general biomechanics studies. It is used extensively in industrial engineering, design offices, research laboratories and technical universities. It has a unique combination of fully integrated multi body and finite element techniques.

MADYMO combines in one simulation program the capabilities offered by multi body, for the simulation of the gross motion of systems of bodies connected by complicated kinematical joints and finite element techniques, for the simulation of structural behavior. It is not necessary to include both in a model, i.e. a model with either finite elements or multi bodies can be used [13]. The multi body algorithm in MADYMO yields the second time derivatives of the degrees of freedom in explicit form. The number of computer operations is linear in the number of bodies if all joints have the same number of degrees of freedom. This leads to an efficient algorithm for large systems of bodies. At the start of the integration, the initial state of the systems of bodies has to be specified (initial conditions). Several different kinematic joint types are available with dynamic restraints to account for joint stiffness, damping and friction. Joints can be unlocked or removed based on a user defined criterion. Planes, ellipsoids, cylinders and facet surfaces can be attached to a body to represent its shape. These surfaces are also used to model contact with other bodies or with finite elements. The contact surfaces are of major importance in the description of the interaction of the occupant with the vehicle interior. The elastic contact forces, including hysteresis, are a function of the penetration of the contact surfaces. In addition to elastic contact forces, damping and friction can be specified.

The output generated by MADYMO is specified through a set of output control parameters. A large number of standard output parameters are available, such as accelerations, forces, torques and kinematics data [13]. MADYMO offers in addition to standard output quantities, the possibility to calculate injury parameters like femur and tibia loads, Head Injury Criterion (HIC), Thoracic Trauma Index (TTI) and Viscous Injury Response (VC). Special output can be obtained through 40 user-defined output routines. Results of the simulation are stored in a number of output files, which are accessible by post-processing programs.

2.6.4. Hyper mesh

Hyper mesh is a finite element modeler used to perform a variety of CAD/CAE tasks including modeling, meshing, and post processing for FEM solvers LSDYNA, NASTRAN, ABAQUS etc. Hyper mesh can be directly used to access the geometric models from leading design software's like CATIA, Pro-E etc. With use of many highly advanced tools presented in Hyper mesh helps to overcome the FEM challenges, including many topological irregularities multi body contacts and others. This has the ability to import geometry from any CAD system and various data exchange standards [21].

Hyper mesh provided with rich set of tools made it possible to achieve a required mesh quality with the different meshing techniques starting from completely automatic solid meshing to thorough node and element creation and editing. It also provided with different types of loads and constraints, which can be applied to either geometric model or to analysis model. The various visualization tools helps to find much critical information, including maximum and minimum values, contour plots which shows trends and correlations. Imaging features such as graphics shading, multiple light sources, local view manipulation and many other sophisticated visualization tools help to speed and improve results evaluation. It is also possible export result images and animation videos in many standard forms which help to present in reports [21].

2.7. Dummy features

The dummy features three main parts, which are head and neck and torso (lower torso and upper torso). The Hybrid III 50th male features a neck design that simulates the human dynamic moment / rotation, flexion, and extension response characteristics of an average size adult male. The shoulder structure was designed for improved fidelity of shoulder belt interaction [13].

Head and Neck

The skull and skull cap are one piece cast aluminum parts with removable vinyl skins. The neck is a segmented rubber and aluminum construction with a center cable. It can incorporate a six axis neck transducer at the top and bottom. This accurately simulates the human dynamic moment/rotation flexion and extension response [14].

Upper Torso

The rib cage is represented by six high strength steel ribs with polymer based damping material to simulate human chest force-deflection characteristics. Each rib unit comprises left and right anatomical ribs in one continuous part open at the sternum and anchored to the back of the thoracic spine [14]. A sternum assembly connects to the front of the ribs and includes a slider for the chest deflection rotary potentiometer. The angle between the neck and upper torso is determined by the construction of the neck bracket which can incorporate a six-axis neck transducer. A two piece aluminum clavicle and clavicle link assemblies have cast integral scapulae to interface with shoulder belts [13].

Lower Torso

A curved cylindrical rubber lumbar spine mounts provides human-like slouch of a seated person and mounts to the pelvis through an optional three axis lumbar load cell. The pelvis is vinyl skin/urethane foam molded over an aluminum casting in the seated position. The ball-jointed femur attachments carry bump stops to reproduce the human leg to hip moment/rotation characteristics. The femur, tibia and ankle can be instrumented to predict bone fracture and the knee can evaluate tibia to femur ligament injury. The foot and ankle simulates heel compression and ankle range of motion [15].

2.8. IIHS (Side Impact Crashworthiness Evaluation Crash Test Protocol)

An injury criterion can be defined as a biomechanical index of exposure severity, which indicates the potential for impact induced injury by its magnitude. There are several kinds of injury criteria's that are related to the human body. These are basically the impact loads acting on the human body. Some of the criteria's pertinent to the Side Impact are discussed here [18].

2.8.1. Head Injury Criterion (HIC)

The Head Injury Criteria is defined as:

$$HIC = \max_{T_O \le t_1 \le t_2 \le T_E} \left[\frac{1}{t_2 - t_1} \int_{t_1}^{t_2} R(t)dt\right]^{2.5} (t_2 - t_1) \quad (8)$$

Where,

T_0= start time of simulation, T_E= end time of simulation and $R(t)$= is the resultant head acceleration in g's measured at head's center of gravity over the time interval T_0< t <T_E. t_1 *and* t_2, are the initial and final times (in sec) of the interval during which the HIC attains a maximum value [17].

HIC36 is used to evaluate head injuries in a side impact and should not exceed 1000 for both the ES-2re and SID-II dummies [17]. A value of 623 is specified as good for the HIC as concussion tolerance level in side (contact) impact. For practical reasons, the maximum time interval t2-t1 that is considered to give appropriate head injury criteria values was set to 36 ms. This time interval greatly affects the head injury criteria calculations, and recently this time interval has been proposed to be further reduced to 16 ms in order to restrict the use of HIC to hard head contact impacts.

2.8.2. Thoracic Trauma Index (TTI)

The TTI is the acceleration criterion based on accelerations of the lower thoracic spine and the ribs. The thoracic trauma index (TTI) provides an indication of the severity of injuries received by motor vehicle occupants in side-impact collision environments. It is the method of quantifying the anatomical extent of the injury, which includes injuries to in tra-thoracic organs. The TTI can be used as an indicator for the side impact performance of passenger cars. The specific benefit of the TTI is that it can be used to address the entire population of vehicle occupants because the age and the weight of the cadaver are included. The TTI is defined by Morgan [17]:

$$TTI = 1.4 \times AGE + 0.5(RIBg + T_{12}) \times \frac{MASS}{MSTD} \quad (9)$$

Where,

AGE = age of the test subject in years, $RIBg$ = maximum absolute value of acceleration in g's of the 4th and 8th rib on the struck side, T12g = maximum absolute acceleration values in g's of the 12th thoracic vertebra, in lateral direction, MASS = test subject mass in kg, MSTD = standard reference mass of 75 kg.

There is also a definition for the TTI that could be used for dummies without a specific age, called the TTI (d). It is defined for 50th percentile dummies with a mass of 75 kg:

$$TTI(d) = 0.5 \times (RIBg + T_{12}g) \quad (10)$$

The dynamic performance requirement, as stated in ENCAP regulations, is that the TTI (d) level shall not exceed 85 g for passenger cars with four side doors and 90 g for two side doors [17].

2.8.3. Pelvic acceleration

The pelvic region consists of the hip joint, iliac wings, sacrum, and pubic rami. The possibilities of pelvic fractures are greater in side impacts. The pubic rami fracture, acetabulum fracture, and hip dislocation are the most commonly caused injuries in a lateral impact. Lateral acceleration from the pelvic region can be utilized to determine whether there are fractures in the pelvic region. According to EURO NCAP, the peak pelvic acceleration (peak lateral sacrum acceleration) shall not exceed 130 g [17].

2.9. EuroNCAP side crash finite element model validation

According to the crash and safety standards approval methods of, crashworthiness and safety of the vehicles shall be assessed by either

- Experimental , full scale crash test or
- Numerical analysis using FE methods

Both methods are considered equivalent and either one may be selected by the vehicle manufacturers for the vehicle approval [3].

Wang Dazhis performed a comparison on both automotive laboratory pole side crash and Finite Element pole side impact simulations. The simulated FE model was validated against the test results. The simulated results were compared in terms of intrusion (deformation) and velocity [4].

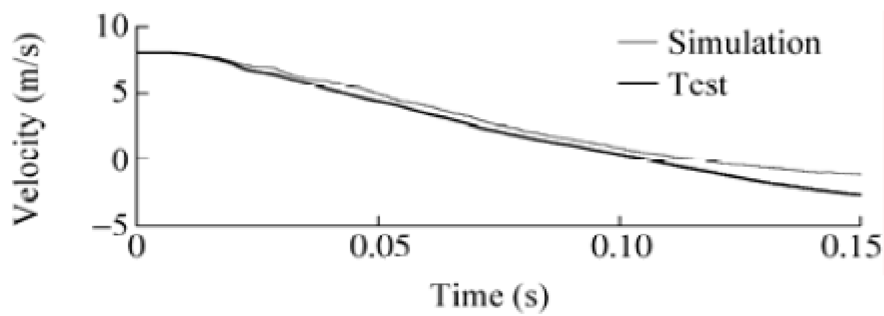

Figure 2.5. Velocity vs. time result of test and simulation of pole side impact

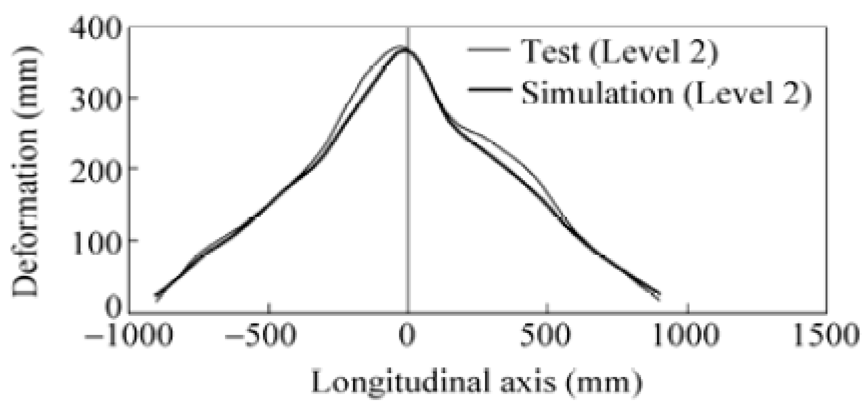

Figure 2.6. Permanent deformation result of test and simulation of pole side impact

The maximum deformation during the impact was larger than the permanent deformation because of the structure spring back behavior, the maximum deformation during the impact was 578mm taken from the motion image analysis.

In addition to that the pole and MDB side impacts were also compared. Although the energy absorbed by both impacts were similar the intrusion level was high in pole side impact due to narrow impact area which resulted to Final conclusion as pole side impact test is highly recommended for better occupant protection [4].

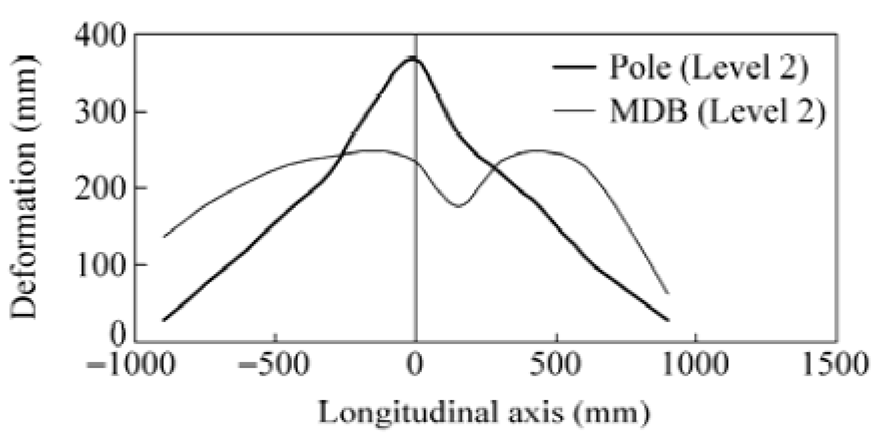

Figure 2.7. Pole vs. MDB permanent deformation

Yao – Jun Zhang [16] studies the crashworthiness of a vehicle b-pillar and door using nonlinear dynamic explicit finite element method and side crash finite element validation is also given. In the study MDB with 50 km/h speed is selected as an Impactor to a stationary vehicle at a simulation time of 140 ms. As a result b-pillar intrusion became 340 mm with a speed of 13 mm/ms (13 m/s).

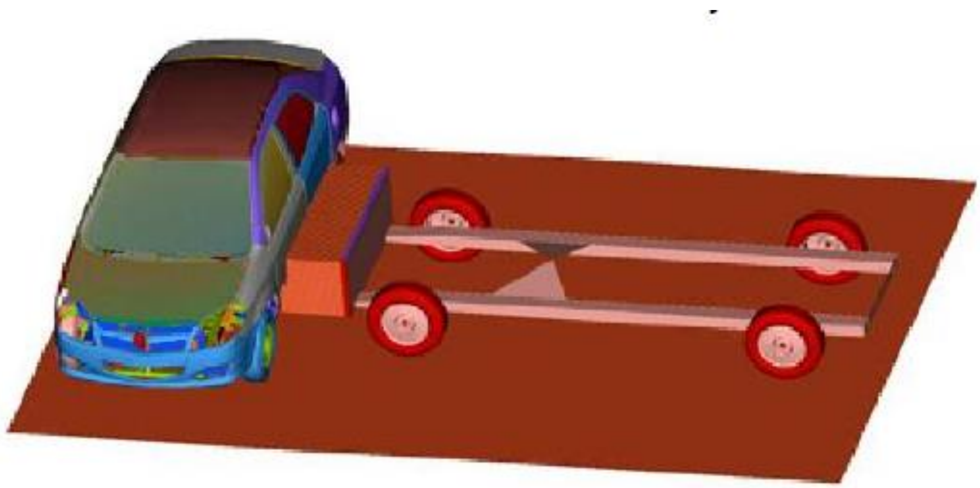

Figure 2.8. Side crash model

Figure 2.9. P, Q, R position

Table 2.1. Intrusion quantity and intrusion speed of three positions

Position	Intrusion quantity (mm)	Intrusion speed (mm/ms)
P	330	15.5
Q	300	14.5
R	340	13.8

Adrian Fails [17] analyzed the body region injury risk ratings for consumers by Euro NCAP from the perspective of real contemporary accidents. Detailed accident cases were analyzed to determine injury and intrusion levels of different vehicles. On this analysis prevention of contact with B-pillar is not sufficient to afford protection to the head in the case of pole side impact. The Peugeot was struck with pole side impact leaving a maximum crash of 730 mm on the B-pillar.

Figure 2.10. Pole-impacted Peugeot 306

CHAPTER THREE

MATERIALS AND METHODS

3.1. Materials

The materials needed to complete this thesis work are

- Steel and composite (carbon fiber material 15) materials with their properties.
- All the necessary dimensions of the Ford Taurus vehicle B-pillar.
- Finite Element model Ford Taurus.
- Finite Element analysis software's such as Hyper Mesh, Hyper Crash, MADYMO and LSDYNA software's to analyze its crashworthiness for occupant safety.

3.2. Methods

In this thesis work different methods are being used to design and analyze the B-pillar.

- Data's about side impact were collected from studies done in Ethiopia. Different literatures were reviewed to study the existing structure of B-pillar of the vehicle. Finite Element model of Ford Taurus is used to analyze the B-pillar for steel and composite materials.
- The internal energy absorbing capacity and intrusion of steel and composite materials are studied in hyper mesh RADIOSS solver, the crashworthiness of the B-pillar assembled with the vehicle is analyzed on hyper mesh.
- The occupant safety of the vehicle with B-pillar that has steel and composite materials will be analyzed by using MADYMO in LS DYNA software.
- Finally the results is discussed using graphs by comparing data's according to Euro NCAP Test Protocol (simulation and experimental) IIHS and experimental test results.

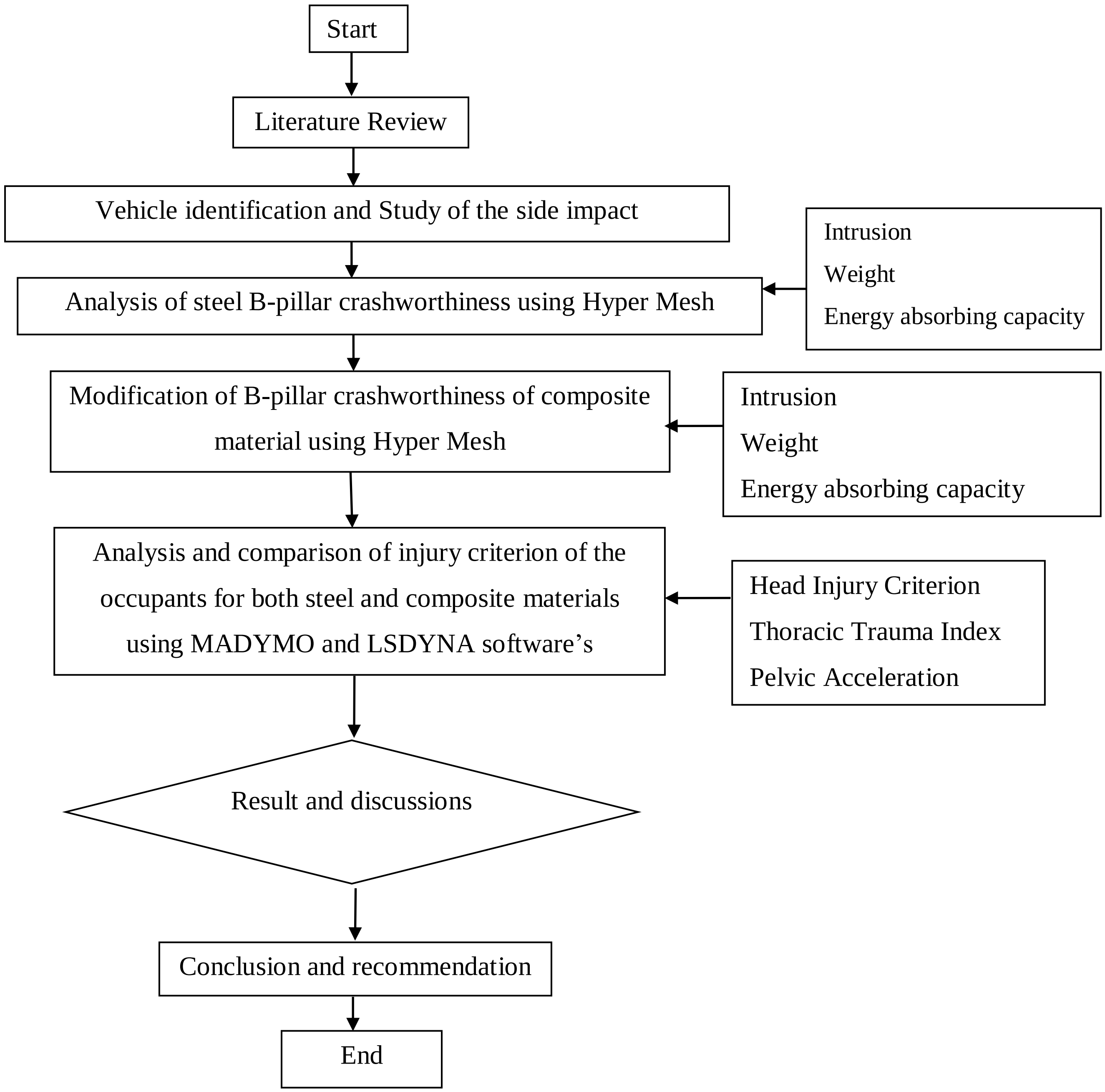

Figure 3.1. Flow chart of methodology

3.3. Side impact modeling and analysis of B-pillar in Ford Taurus

3.3.1. Design of B-Pillar

B-pillars are one of the most sophisticated parts of the automobile body, because this component has to comply with lot of requirements and specifications. The distance between the B-Pillar and the occupant is very less in side impact when compared to the frontal impact. In addition, when the impact occurs, the B-Pillar or structures in the B-Pillar have to absorb more energy with minimal acceleration to the occupant [12]. The rectangular B-pillar has a dimension of 1120 mm length and 900 mm width and 2mm thickness for steel material.

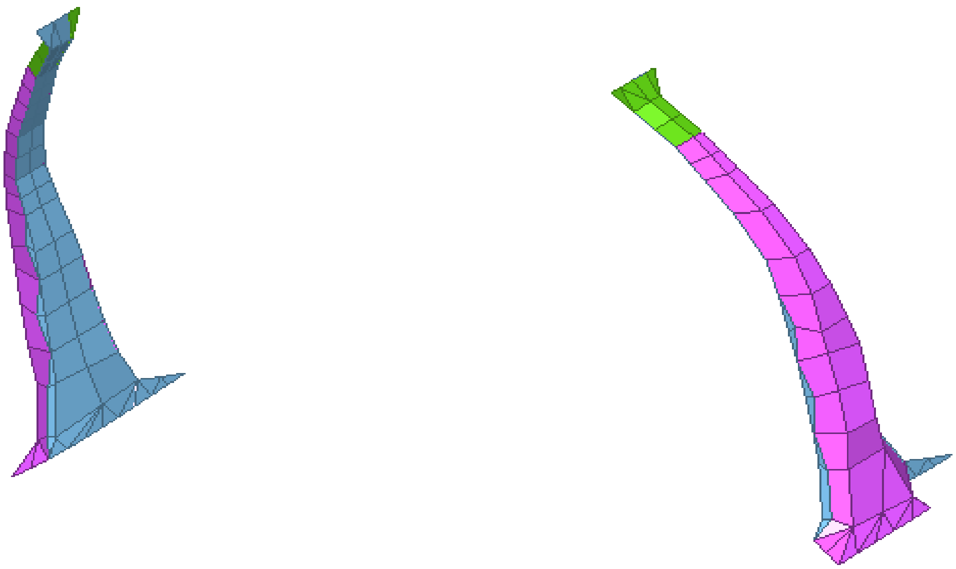

Figure 3.2. B-pillar of ford Taurus

The new design as in figure 3.2 is intended to use carbon fiber composite structures to generate significant weight savings for an automobile. The first phase was a structural design study.

3.3.2. Material description

The carbon fiber composites are light weight material because of its low density. The mechanical properties of the carbon fiber are very much suitable as they have high impact energy absorption before fail and also they have high strength requirements.

Table 3.1. Material properties of steel [23]

Mass Density	7.8 g/cc
Young’s modulus	210 GPa
Poison’s Ratio	0.3
Yield Stress	0.215GPa

Table 3.2. Material properties for carbon fiber laminate mat 15 [23]

Mass Density	1.58 g/cc
Longitudinal Modulus E1	144GPa
Transverse Modulus E2	10.3GPa
In plane Shear Modulus G12	7.2GPa
Poisson’s Ratio	0.25
Longitudinal Tensile Strength F1t	1830Mpa
Transverse Tensile strength F2t	57MPa
In plane shear Strength F6	71MPa
Longitudinal Compressive Strength F1c	1096MPa
Transverse Compressive Strength F2c	228Mpa

The mechanical properties of the carbon fiber composites can be changed according to the requirements by changing orientation of the fiber in the loading direction, layer stacking and by changing the volume fraction of the fiber and the matrix. The material properties of steel and Carbon Fiber laminate are shown in Tables 3.2 and 3.3.

Carbon fiber composite can sustain the same load as of steel even with the 57.2 percent of the steel weight. The carbon fiber composites have very high specific strength and specific stiffness when compared to steel.

3.3.3. Thickness and orientation of composite B-pillar

Thickness of the structure plays a vital role in energy absorption of a material. By increasing the thickness, the structure can be made to withstand more loads and thus more energy absorption. However, the volume also increases when there is any increase in thickness and this in turn increases the mass of the structure. This not acceptable in the field of automotive engineering because in crashworthiness as weight plays a very critical role in increasing the fuel efficiency of the vehicle. In this study, thickness is varied to 1.6 mm and 4.15 mm. When the 1.6 mm thickness is used, the deformation is very much and the deformation pattern is completely different. In addition, the von mises stress and strain is very high. The 4.15 mm thickness yielded very good stress and strain value. Therefore, 4.15mm thickness is used in every composite part once thickness is decided; the next step is to find a the orientation that has less deformation, stress and strain by varying the thickness from 1.6 to 4.15 mm, the pillar must be subjected not less than 100 KN to analyze its different properties [6]. In this design a load of 140 KN is applied in order to analyze the deformation, stress and strain properties the pillar.

Ply Orientations used

a. 0°,90°,45°,90°,0°
b. 0°,45°,0°,45°,0°,45°,0°,45°,0°
c. 0°,30°,-30°,60°,-60°,90°,0°,90°,-60°,60°,-30°,30°,0°

Table 3.3. B-pillar thickness set to 1.6 mm

Ply Orientation	Ply thickness	Intrusion (mm)	v.stress (MPa)	v.strain (MPa)	Composite failure
A	0.32	9.828	59.35	3.98e-03	5.534e-01
B	0.177	10.07	55.89	3.99e-03	6.404e-01
C	0.13	8.79	56.63	3.81e-03	5.501e-01

Table 3.4. B- Pillar thickness set to 2.9 mm

Ply Orientation	Ply thickness	Intrusion (mm)	v.stress (MPa)	v.strain (MPa)	Composite failure
A	0.58	3.332	34.12	2.273e-03	2.024e-01
B	0.32	3.3795	32.36	2.161e-03	2.241e-01
C	0.22	3.396	34.84	2.322e-03	2.196e-01

Table 3.5. B-pillar thickness set to 4.15 mm

Ply Orientation	Ply thickness	Intrusion (mm)	v.stress (MPa)	v.strain (MPa)	Composite failure
A	0.83	1.953	24.5	1.626e-03	1.172e-01
B	0.46	1.917	23.27	1.548e-03	1.548e-01
C	0.32	1.945	24.78	1.645e-03	1.645e-01

As it is seen from the above tables a deformation of 10.07 mm is attained when the thickness is set to 1.6 mm. but when the thickness is set to 4.15 mm the deformation is 1.917 mm. similarly the stress and strain values decrease when the thickness is increased from 1.6 mm to 4.15 mm. Therefore the thickness 4.15 mm is selected. After selecting the thickness the ply orientation has to be selected. On the other hand the ply orientation showed relatively small differences; still ply orientation 0°,45°,0°,45°,0°,45°,0°,45°,0° is selected because it has relatively better results of deformation, stress and strain when compared to the other orientations.

This study proposed variable thickness panels to maximize the structural efficiency at minimum mass. The wall thickness is constrained to be at 4.15mm. For the structural analysis of the B-Pillar, Hyper Mesh Optistruct solver was used since it is the most widely used computational method for composite materials in the automotive industry.

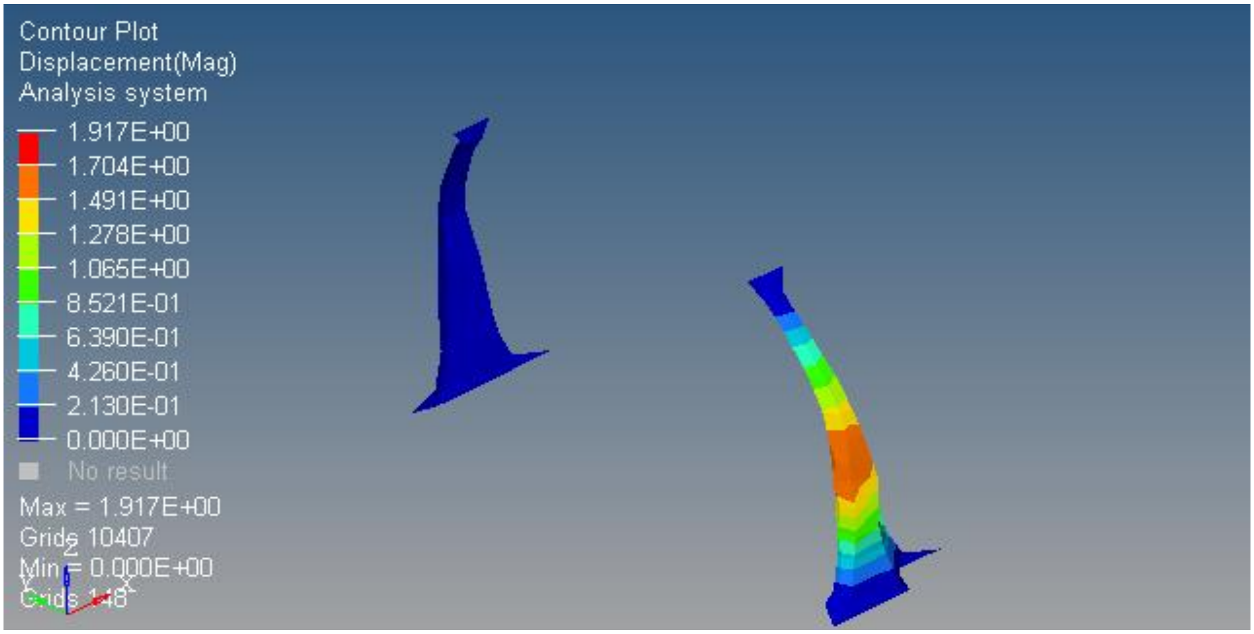

Figure 3.3. Deformation of B-pillar

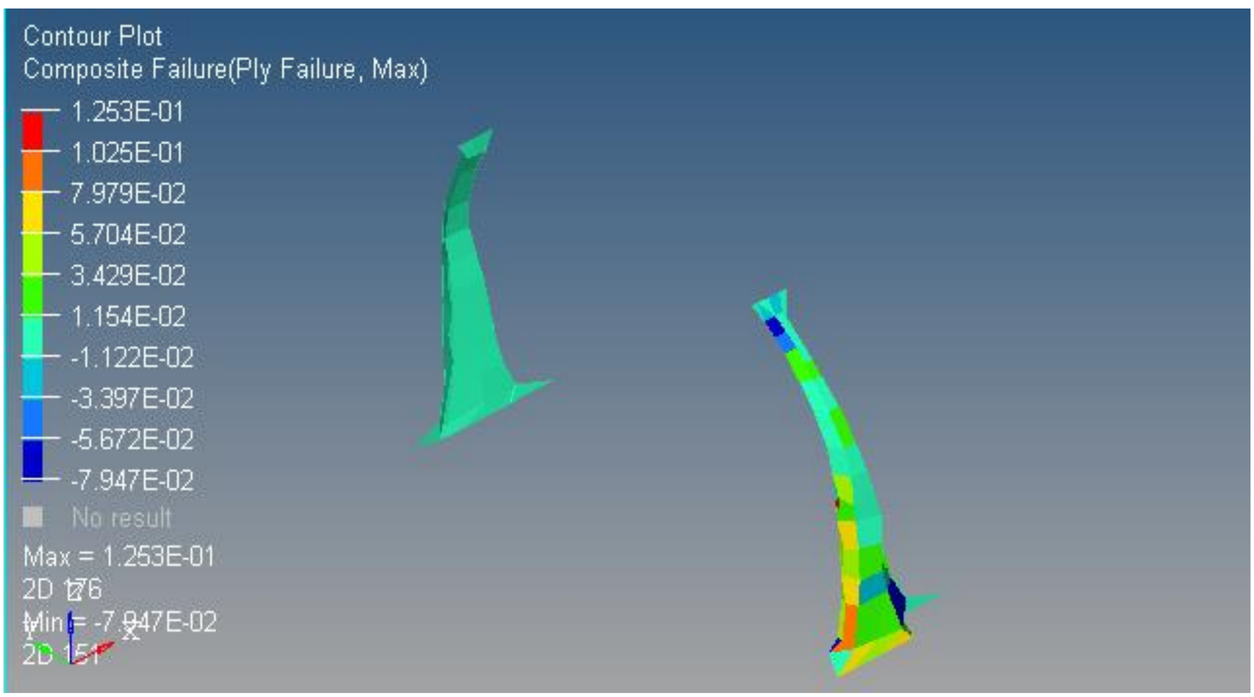

Figure 3.4. Composite failure of B-pillar

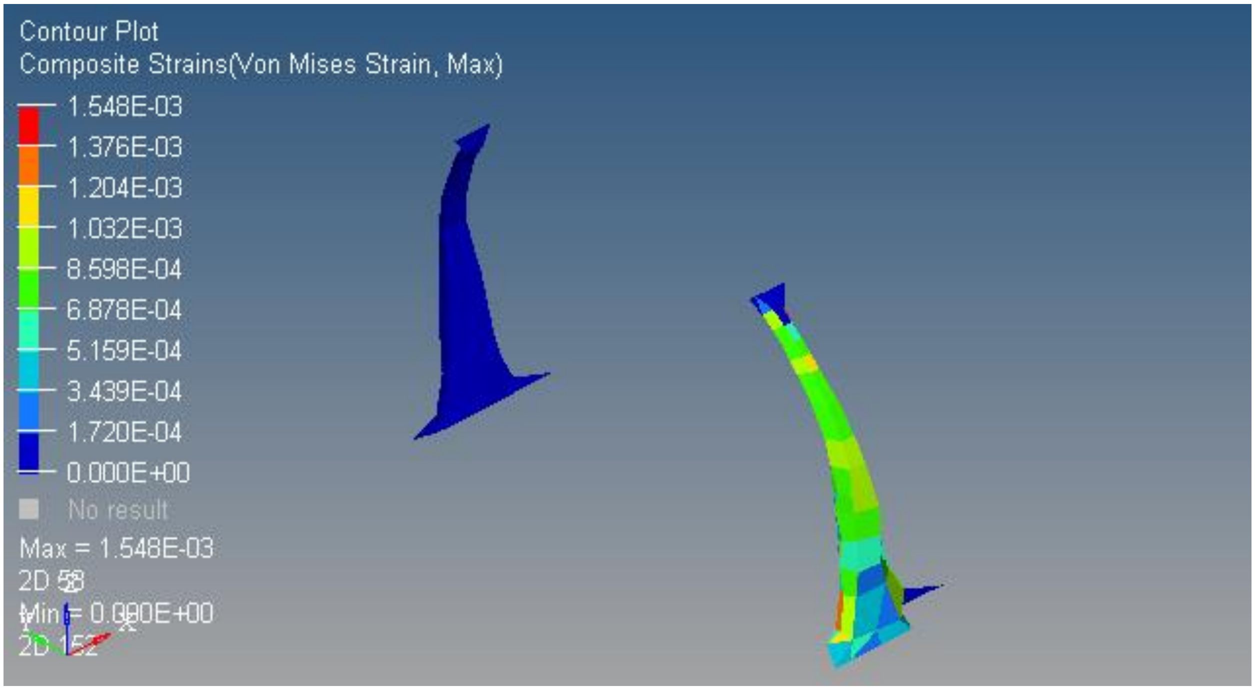

Figure 3.5. Max von mises strain of B-pillar

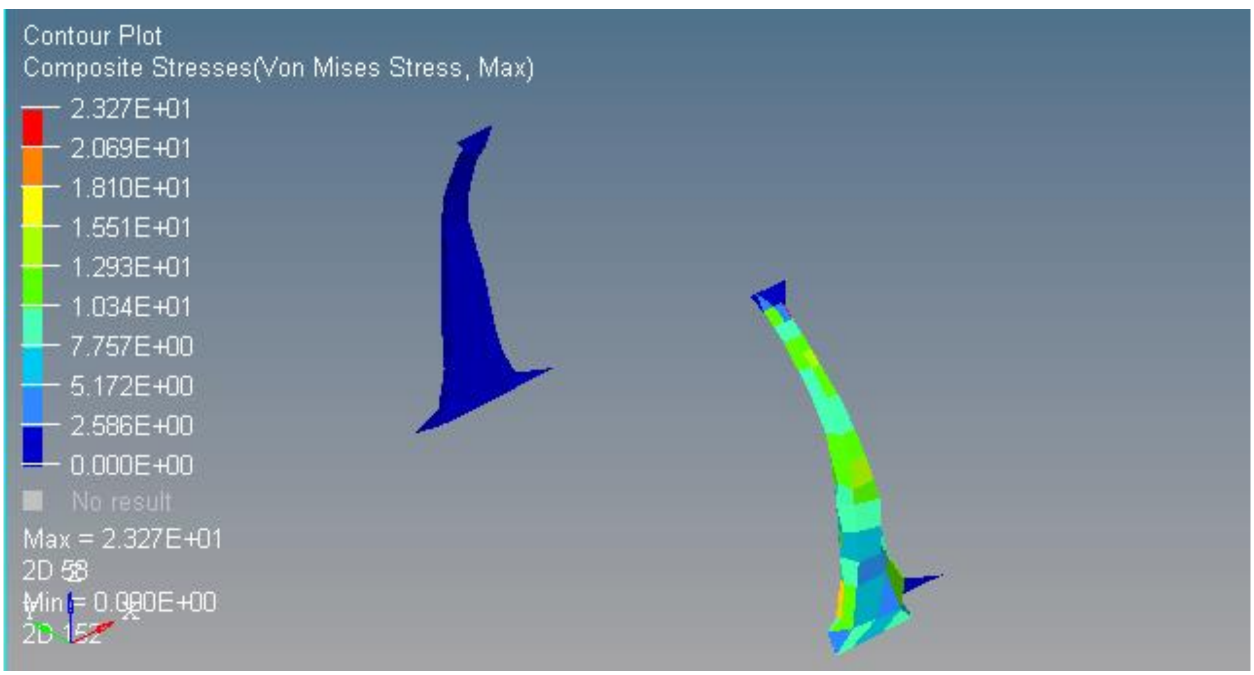

Figure 3.6. Max von mises stress of B-pillar

The above figures give a basic description of the B-Pillar with composite as the material. In this model shell elements are used with the number of plies to be 9 with each ply thickness to be 0.46 mm each. The number of nodes and elements present are shown in Table 3.6. The weight of the composite B-Pillar is reduced drastically when compared to the steel B-Pillar. The weight of the composite B-Pillar is 1.1 kg whereas the weight of the steel B-Pillar made of steel is 2.6 kg. The weight of the composite is 57.9% less when compared to the steel B-Pillar. This shows the weight reduction when a composite material is used.

3.3.4. Properties of B-pillar

Table 3.6. Properties of B pillar [22]

Number of Nodes	433	- - - -
Number of Elements	754	- - - -
Material	Carbon fiber	Steel
Thickness	4.15mm	2mm
Weight	1.1kgs	2.6kgs

3.3.5. Analytical verification of B-pillar

Consider 1625 kg vehicle mass traveling at 29Km/h is colliding with a pole or rigid barrier on its B-pillar get crash. Carbon/Epoxy composite B-pillar dimensions except the thickness are the same with the steel: where L (length) =1120mm, W (width) = 900mm, and T (thickness) = 2.00mm for steel and 4.15mm for composite side impact beam as well as B-pillar. B-pillar absorbs the impact energy through deformation. Kinetic energy [22],

$$K_E = \frac{1}{2}mv^2$$

$$K_E = \frac{1}{2}1625kg(29km/h)^2$$

$$K_E = 527242Nm$$

Where, KE is kinetic energy, m is mass of the vehicle and v is initial velocity of the vehicle

Composite stress

Stress is calculated using the following equation when a load of 140 KN is applied to the pillar [19].

$$\sigma = \frac{F}{A}$$

$$where\ A = l \times w \times t\ for\ rectangular\ pillar\ and\ F = 140\ KN$$

$$A = 0.006361m^2$$

$$\sigma = \frac{140000}{0.006361}$$

$$\sigma = 22.009\ MPa\ similar\ with\ the\ Hyper\ Mesh\ value = 23.27$$

Where, σ is stress, F is applied force and A is area of the circular B-pillar

Composite strain

The strain is calculated according to the following equation where the young's modules of the carbon fiber is taken to be 144GPa [22],

$$\varepsilon = \frac{\sigma}{E}$$

$$\varepsilon = \frac{22.009}{144000}$$

$$\varepsilon = 1.528 \times E^{-3} MPa$$

Where, σ is stress ε is the strain value and E is young's modules

Deformation (displacement)

The deformation value determined after 140 KN load is applied to the pillar can be calculated using the change of deformation equation [22].

$$\varepsilon = \frac{\Delta L}{L}, where\ \Delta L = \varepsilon \times L$$

$$\Delta L = 1.528 \times E^{-3} \times 1120$$

$$\Delta L = 1.711mm\ which\ is\ simillar\ with\ the\ optistruct\ value\ \Delta L = 1.917mm,$$

$$which\ is\ simillar\ with\ the\ software\ result$$

Where, ΔL is change in length and L is original length

Percentage of mass saving in B-pillar [22]

$$\text{\% of mass saving} = \frac{(\rho \times volume) of\ steel - (\rho \times volume)\ of\ carbon\ fiber}{(\rho \times volume) of\ steel} * 100$$

$$\text{\% of mass saving} = \frac{(7.8cc \times 1.272cc) of\ steel - (1.58cc \times 2.64cc)\ of\ carbon\ fiber}{(7.8cc \times 1.272cc) of\ steel} * 100$$

$$\text{\% of mass saving} = 57.957\%$$

Where, ρ is the density of the material.

Total mass of the composite is 57.957% less when compared to the total mass of the steel B-pillar and absorb more deformational energy. Thickness of the composite B-pillar is of 4.15 mm in order to maintain the equivalent stiffness and energy absorption.

3.4. Side impact modeling and analysis of B-pillar in a Ford Taurus

3.4.1. Finite element study of Ford Taurus

Due to the increasing cost of conducting an experiment, finite element models are used everywhere. Automotive industry is the filed, which utilizes the FEM to the most. Finite Element Models are accurate to simulate several different crash tests and predict the vehicle and occupant response various crash scenarios. Such a design leads to minimize the time and the cost of the testing process and helps in making effective safety decisions. The Ford Taurus model used for the analysis is a four-door sedan with 5 meters length, 2.76 m wheelbase and weighs 1625kg. It is developed by NHTSA. Figure 3.7. shows the finite element model of Ford Taurus Model. It has 134 parts, which represent different vehicle parts and these parts are joined by rigid body constrained options and spot-weld. The contacts between different parts are modeled as single surface sliding interface (AUTOMATIC_SINGLE_SURFACE).

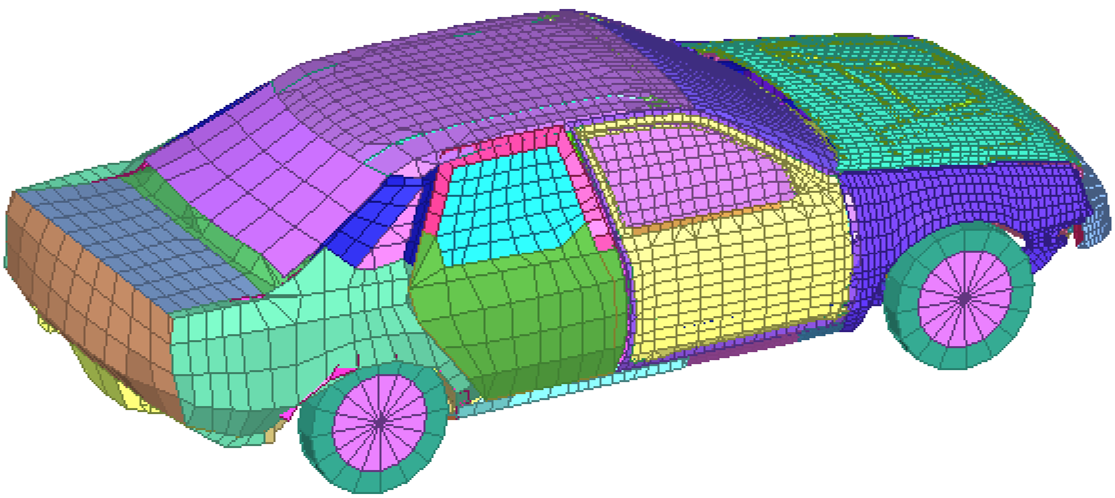

Figure 3.7. Ford Taurus finite element model

Table 3.7. Finite element summary of Ford Taurus [22]

Number of Parts	134
Number of Nodes	26797
Number of Quad Elements	23124
Number of Tri Elements	4750
Number of Hexa Elements	338
Number of Penta Elements	10

The above table depicts the finite element summary of Ford Taurus. It consists of 134 parts and these represent the different parts of the vehicle. Two different types of shell elements are used, triangular and quadrilateral. This model consists of shell B-Pillar and the solid elements. The shell elements have isotropic elastic plastic material and eight stress strain points define the stress strain relationship. B-Pillar elements are assigned with isotropic elastic material and the solid elements have honeycomb material with constant stress element formulation.

3.5. Impactor modeling

The pole side impact test, according to Euro NCAP pole side impact test protocol. The test vehicle is placed on a large planar trolley, which allowed the free motion of the vehicle to be no less than 1 m. The trolley and the vehicle are accelerated together to 29 km/h, impacting a 254-mm diameter rigid cylinder pole. The impact position aimed at the center of the gravity (C.G.) for the dummy head. Thornton and Edwards conducted a study investigating the geometrical effects in energy absorption of circular, square, and rectangular cross section tubes. They concluded that for a given fiber layup and geometry, the specific energy follow the order, circular>square>rectangle.

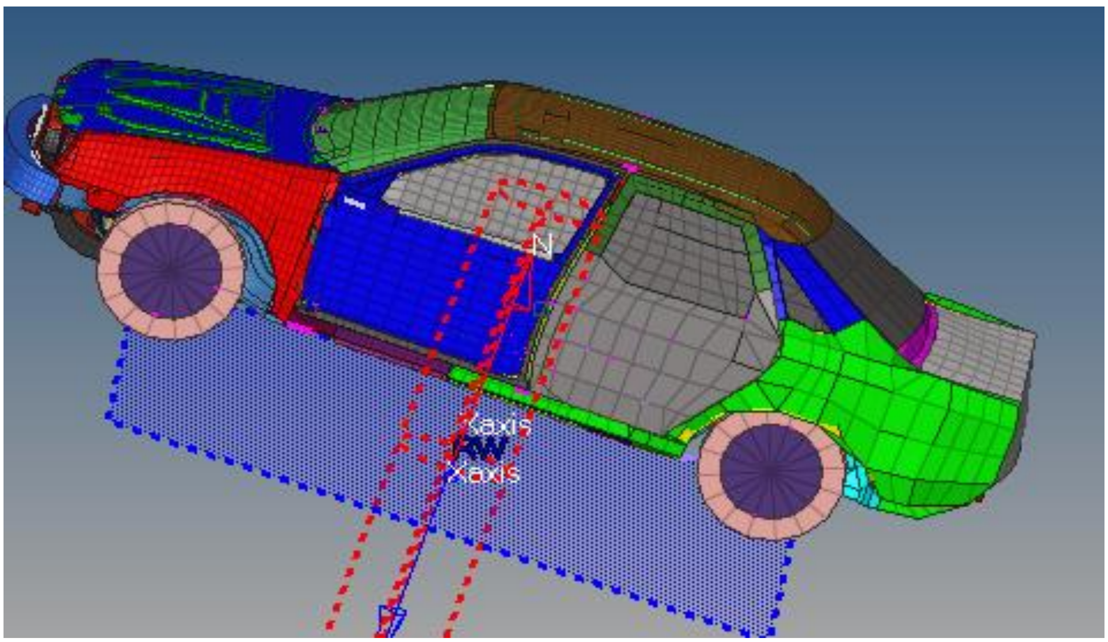

Figure 3.8. Side Impact pole and vehicle

3.6. Hyper mesh simulation

According to Euro NCAP pole side impact test protocol, the vehicle moves in the direction of the pole and strikes the pole with the driver side of the car at an angle of 90° with the velocity of 29 km/h. The distance between the vehicle and the pole is kept to the minimum in order to minimize the simulation time [15].

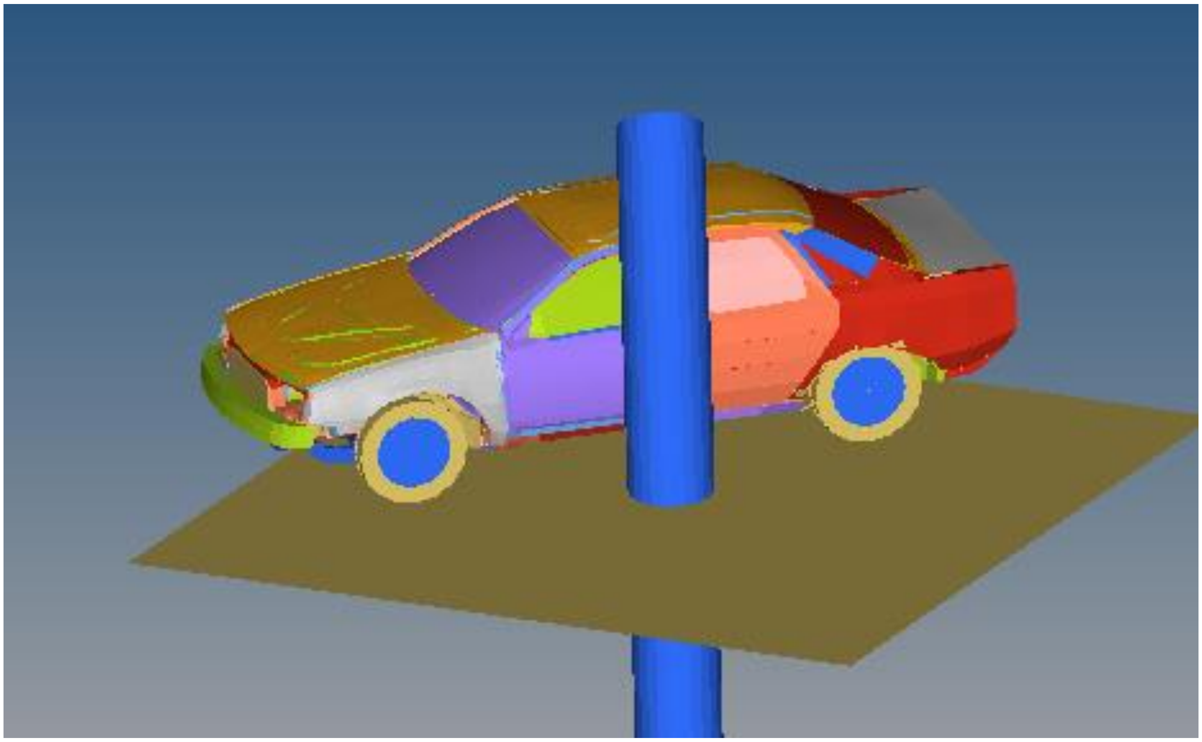

Figure 3.9. Pole crash sequence at t = 0.00s

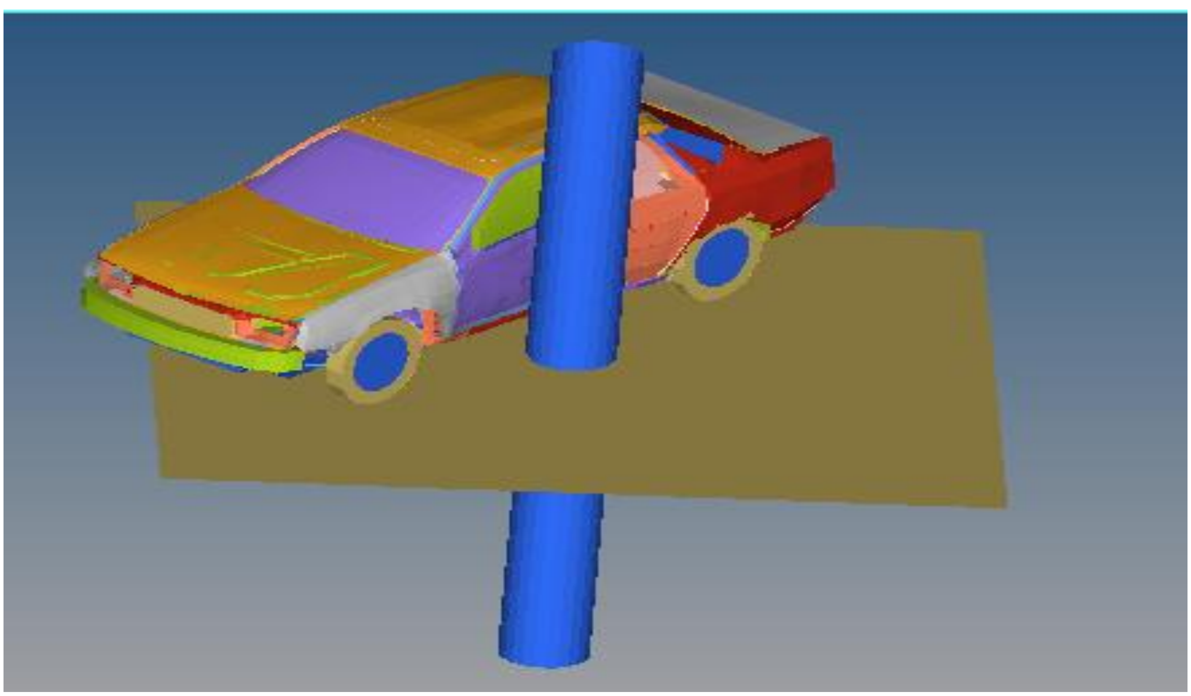

Figure 3.10. Pole crash sequence at t = 0.033s

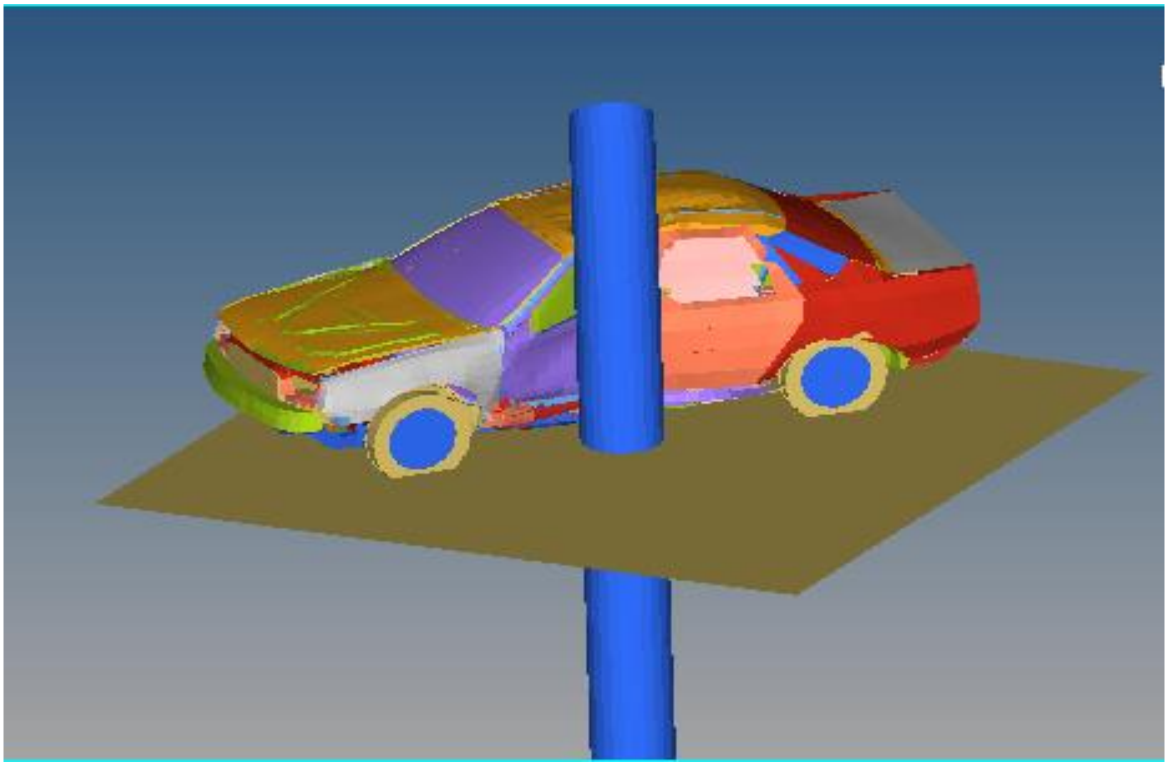

Figure 3.11. Pole crash sequence at t = 0.09s

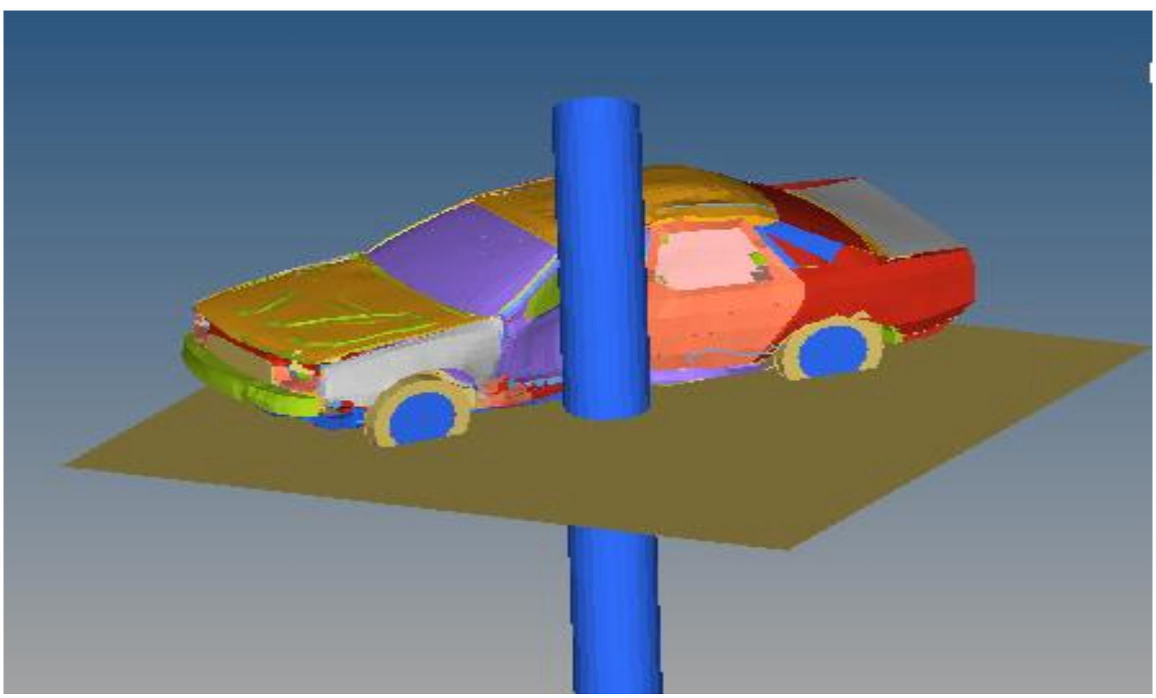

Figure 3.12. Pole crash sequence at t = 0.15s

This simulation is run for 0.15s and figures 3.9-3.12, shows animation sequences of the side-impact crash analysis According to the figure 3.9-3.12, it can be noticed that there is considerable deformation sustained by the Ford Taurus sedan. The pole passes all its energy into the side door of a car. As a reason the B-pillar and side door of the car should have the ability to withstand the load so that there is less injury on the occupant of the vehicle.

3.7. Analysis of B-Pillar

The new B-Pillar with carbon fiber is placed in the car. Hyper Crash is used to merge the B-Pillar with the car. Hyper Crash is also used to assemble the newly designed side-impact B-Pillar. This analysis is done using Euro NCAP pole side impact test protocol. First of all Euro NCAP pole side impact test protocol is used to study the deformation sustained by the car when using the new designed B-Pillar. It has already been decided earlier in this study that carbon fiber composite is stronger and absorbs more energy. In this chapter, this is proved again by merging the new modeled composite B-Pillar in the car. In addition, steel results are also included to help in interpreting the results. As discussed earlier, in this test the vehicle is made to impact the stationary rigid pole at a speed of 29 km/h. The vehicle moves at an angle of 90° [15].

3.7.1. Simulation of side impact crash with the present steel B-Pillar

The full Side Impact model is carried out in hyper mesh for 0.15 seconds. The accelerometers are placed at eight locations (near the driver side) in the vehicle. The contacts are defined by geometric interface. Figure 3.13 shows the deformation sustained by the pillar when the vehicle is crashed in to the rigid pole; whereas Figure 3.14 shows the velocity of the vehicle at which the deformation occurs.

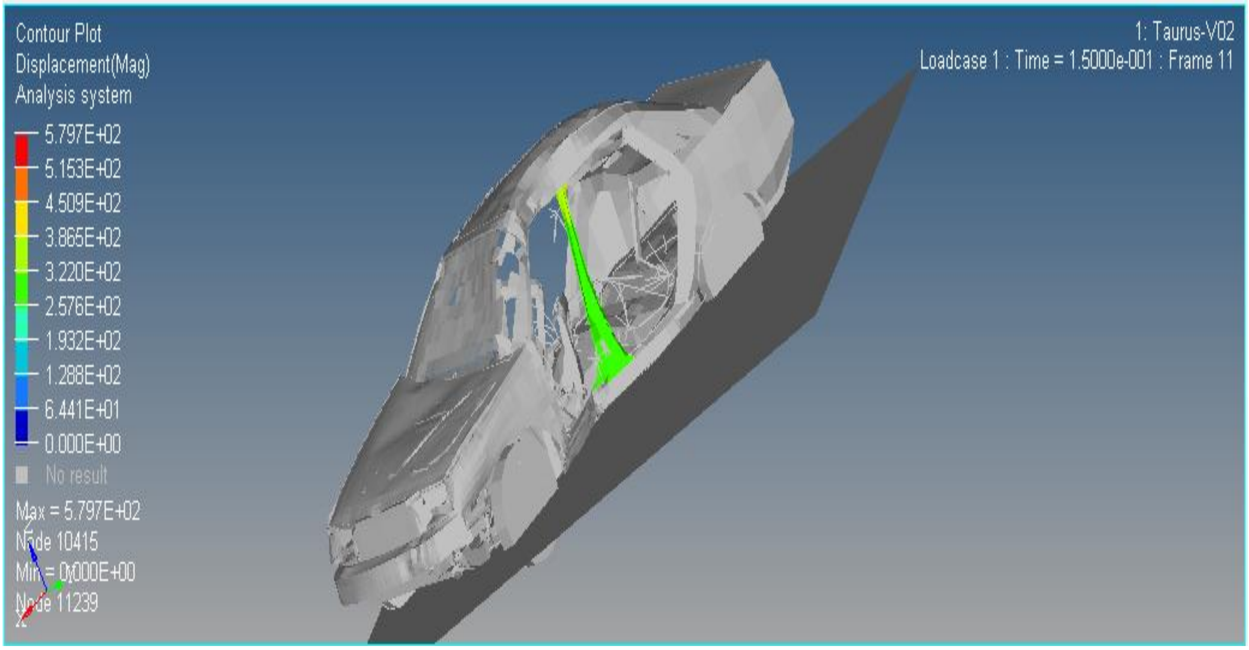

Figure 3.13. Displacement of steel B-pillar at t=0.15s

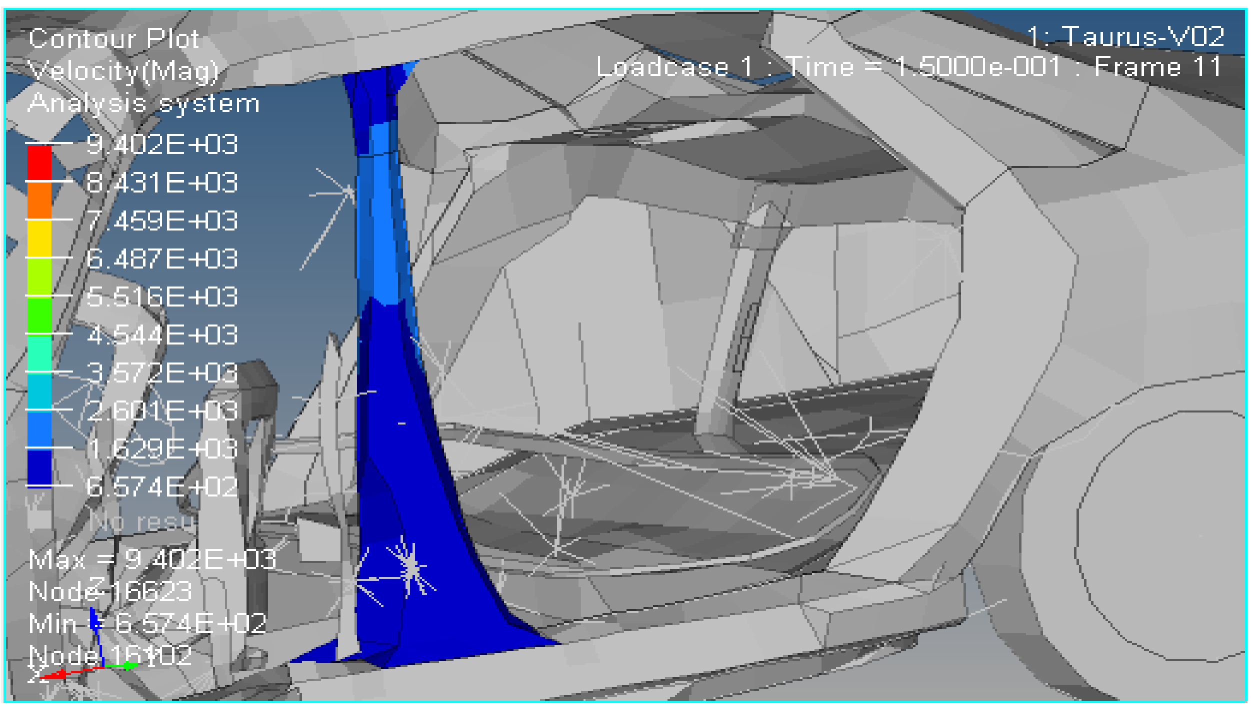

Figure 3.14. Velocity of steel B-pillar at t=0.15s

3.7.2. Simulation of side impact crash with Composite B-Pillar

The present B-pillar in the Ford Taurus car was removed using Hyper Crash and the composite B-Pillar was merged with car. Deformation sustained by the car while using the carbon fiber reinforced composite B-Pillar is shown in figure 3.15; whereas figure 3.16 shows the velocity of the vehicle at which the deformation occurs.

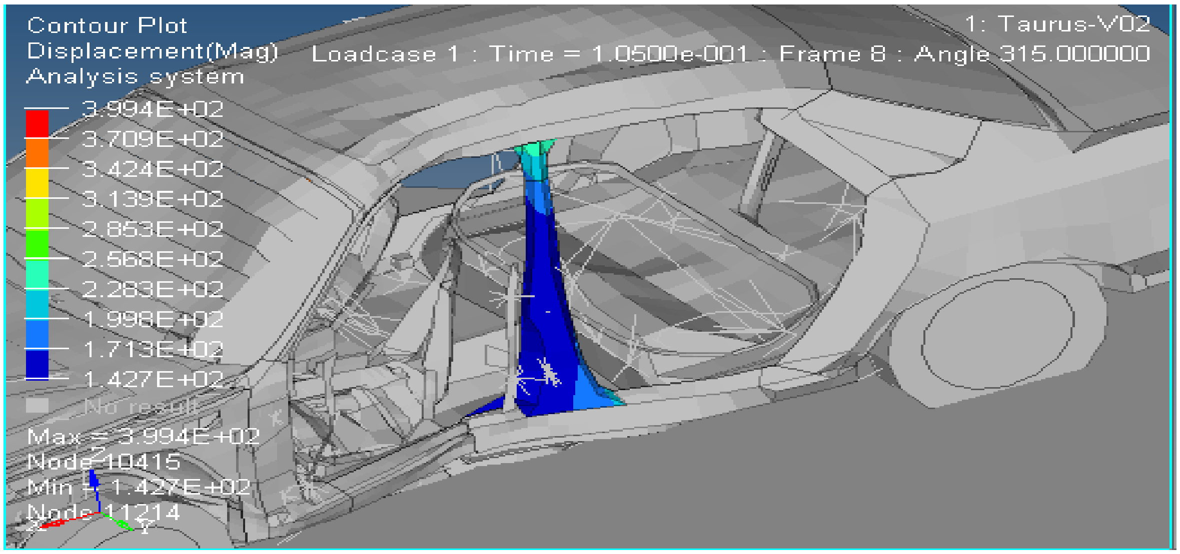

Figure 3.15. Displacement of composite B-pillar at t=0.15s

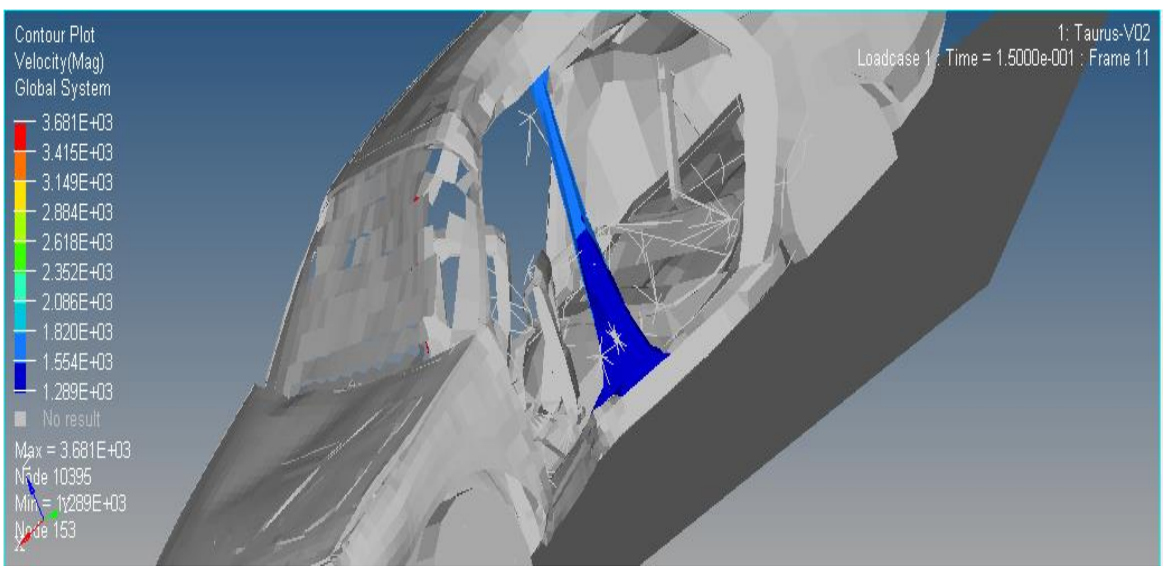

Figure 3.16. Velocity of composite B-pillar at t=0.15s

3.8. Internal energy absorption of steel and composite materials

Table 3.8. Material Energy Absorption

Steel	31 MJ
Carbon Fiber	62.5 MJ

The above table shows energy absorbed by different materials. Results are compared and the best material is selected for the B-Pillar. In this case carbon proved out to be the best material as the energy absorption of carbon is twice as that of steel which is the original material. The thickness of carbon fiber is 4.15mmand is made of shell elements. Figure 3.17 and 3.18 shows time vs. internal energy and kinetic energy of steel and carbon fiber B-pillars. Internal energy of the material specifies the ability of the material to withstand the load while it is deformed. The higher the internal energy the higher the ability of the material in taking the load. Therefore the energy absorption of the material increases. From figure 3.17 and 3.18 the end time specific energy absorption of carbon is very high when compared to steel. Thus, it can be concluded that carbon fiber has higher energy absorption. Therefore, these are the parameters considered when analyzing the B-Pillar.

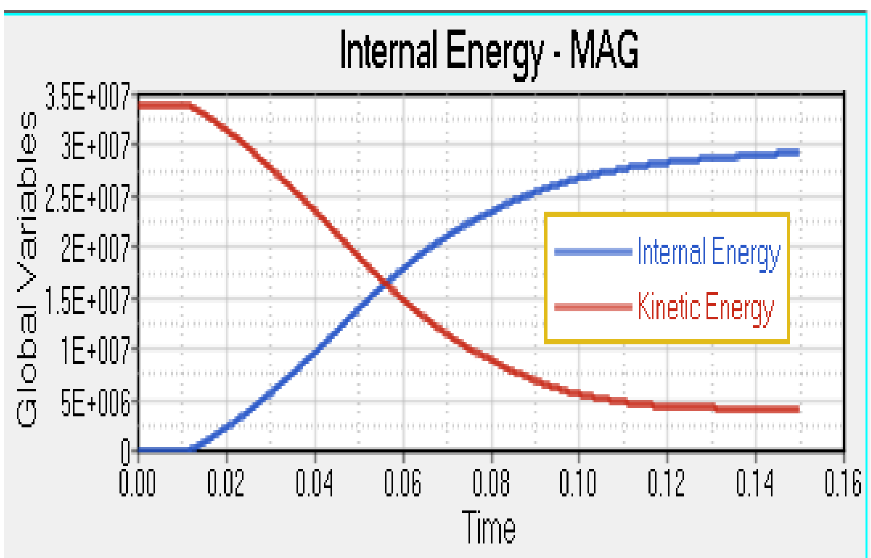

Figure 3.17. Specific energy of steel B-pillar

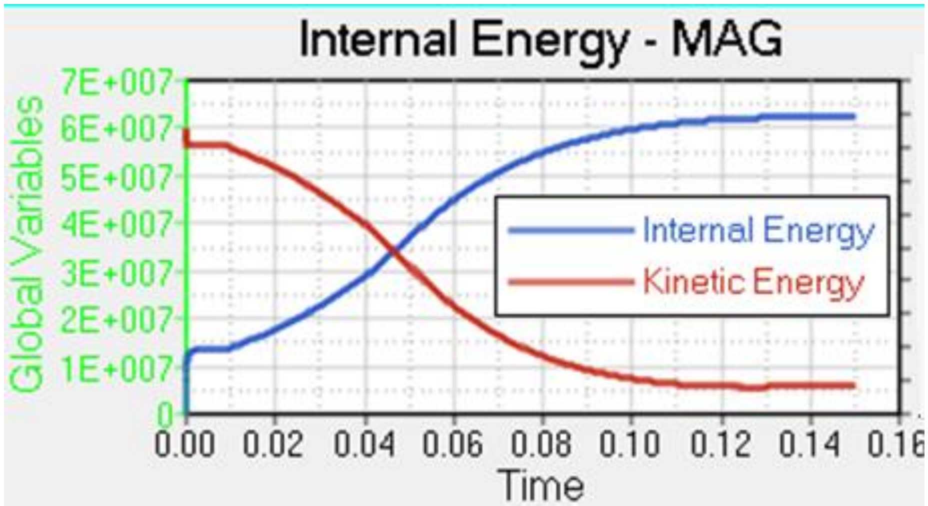

Figure 3.18. Internal energy of composite B-pillar

3.9. Occupant bio-dynamic modeling and potential injury

3.9.1. MADYMO Modeling

Crashworthiness and occupant injury simulations are often used to evaluate the effectiveness, and potential limitations of proposed test procedures and safety countermeasures. Safety of occupant is the most important issue that concerns during the design and development of vehicle [21].

3.9.2. Dummy models

To simulate a human being in crash scenario MADYMO dummy models are used. Two MADYMO model types are available as shown in figure 3.19. These model types are Ellipsoid models and Finite Element models. Ellipsoid models are models that are based fully on MADYMO's rigid body modeling features. Their geometry is described by means of ellipsoids, cylinders and planes. They are the most CPU-time efficient type of models. Therefore, they are particularly suitable for concept, optimization and extensive parameter sensitivity studies. A wide range of MADYMO models are available. The standard models of the adult and child Hybrid III dummies are the 5th percentile female, the 50th percentile male, the 95th percentile male, 6-year-old child and 3-year-old child Hybrid III dummy models. The size and weight of the Hybrid III 50th percentile male represents an "average" of the American adult male population. In order to cover the adult population two other versions of the Hybrid III have been developed, the 5th percentile small female and the 95th percentile large male [21].

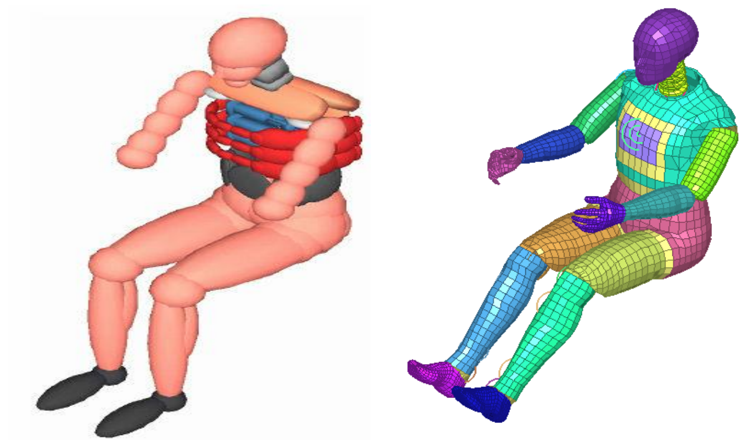

a, Ellipsoidal dummy model b, FEA dummy model

Figure 3.19. Dummy models

The above figure shows the ellipsoidal and FEA dummy models. Hybrid III 50th percentile dummy is the most widely applied dummy for the evaluation of automotive safety restraint systems in frontal and side crash testing. The EUROSID-1 Side Impact Dummy has been designed to represent a 50th percentile adult male subject during side impact crash conditions. It is used in European and Japanese side impact test procedures. The Euro SID is a lateral impact dummy which is specified in the 96/27/EG directive for the protection of motor vehicle occupants [13]. The standard Hybrid III 50th percentile dummy as shown in figure 3.20 has been developed for seated automotive applications. The standing Hybrid III contains some adapted parts and thereby has a wider range of application including standing and testing pedestrian accidents.

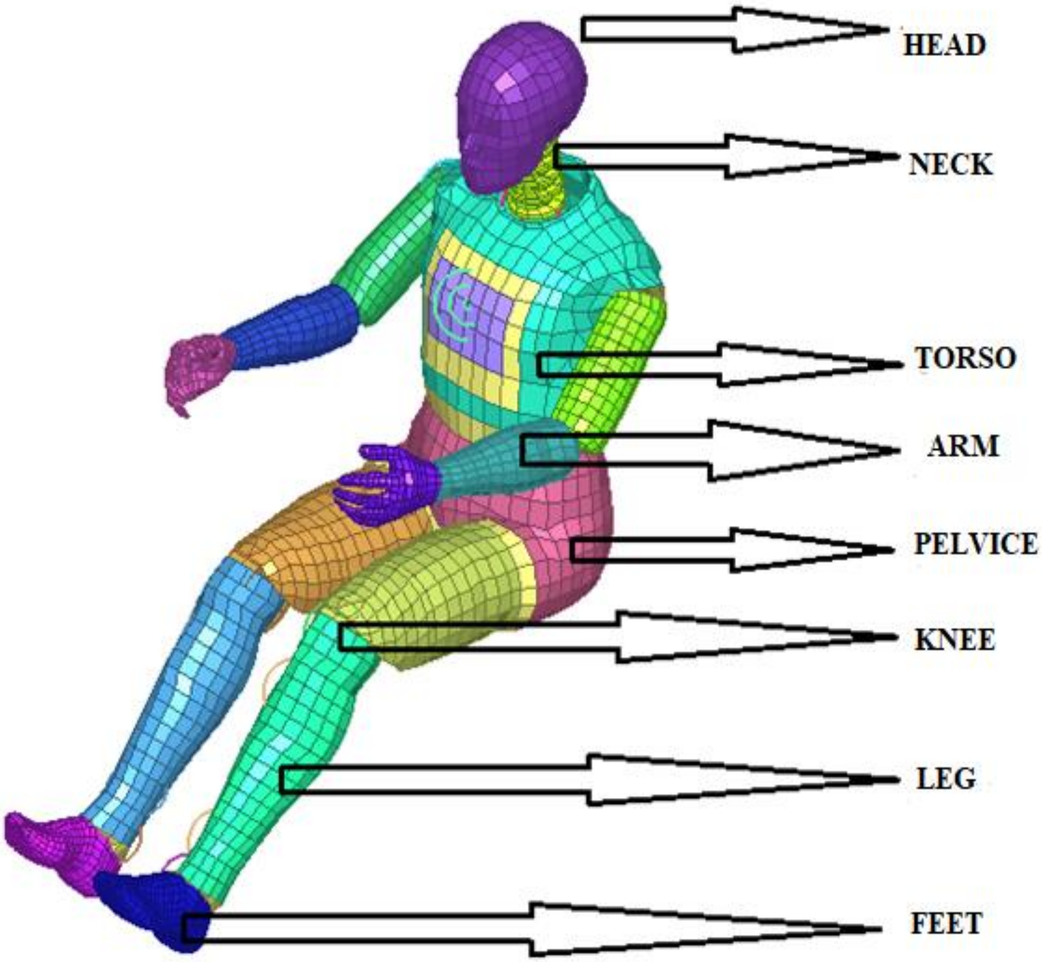

Figure 3.20. Hybrid III 50th percentile dummy

Table 3.9. Weight of Hybrid III 50th percentile side impact dummy [13]

Weight	78.22 kg
Stature	1752 mm (1.75 m)
Sitting Height	883.92 mm

Table 3.9 shows that the weight, stature and sitting height of the Hybrid III 50th percentile side impact dummy. Their geometry is described by means of ellipsoids, cylinders and planes. Segmented weights of each part from head to feet are shown in Table 3.10.

Table 3.10. Segmented weights [13]

Part weight	**Kg**
Head	4.54
Neck	1.54
Upper torso	17.2
Lower torso	23.06
Upper arms	3.99
Lower arms and hands	4.54
Upper legs	11.98
Lower legs and feet	11.35
Total weight	78.22

Table 3.11. External dimensions for the hybrid III 50th percentile male [13]

Dimension description specification	**Mm**
Head circumference	596.9
Head breadth	154.94
Head depth	203.2
Erect sitting height	883.92
Shoulder to elbow length	337.82
Back of elbow to wrist pivot length	297.18
Buttock to knee length	591.82
Knee pivot height	495.3

The above table shows the dimension of each of the parts in the Hybrid III 50th male dummy. Here the head circumference, breadth and depth are taken from an average American adult male population.

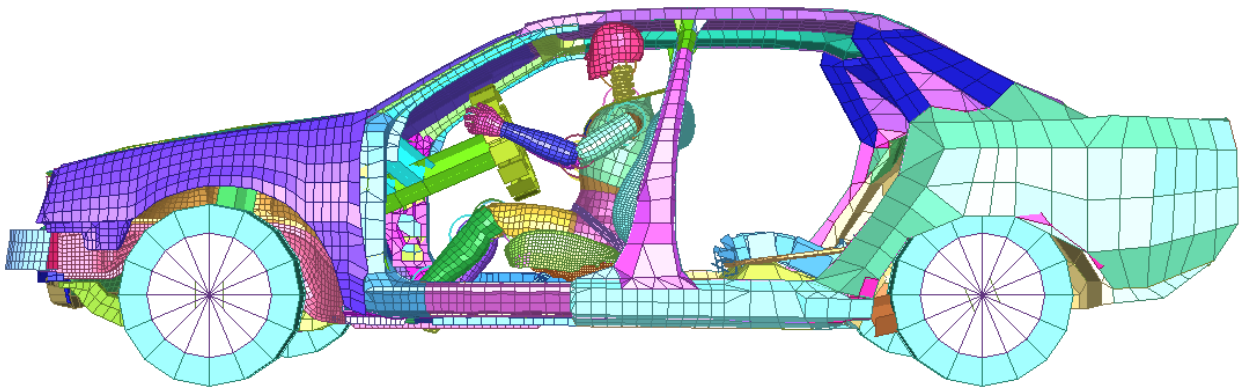

Figure 3.21. Hybrid III 50th male dummy merged with Ford Taurus

3.9.3. Simulation

In this study Hybrid III 50th percentile side impact dummy model is used as the reference model. Seat belts play a vital role in reducing the injuries of the occupant. Here the seat belts developed in MADYMO 601 are classified as FEM belts. These are basically the three-point belt restraint system. The width and thickness of the belt are equal to 40mm and 1mm respectively. Belts are modeled with 0.02 size tri-elements. HYSISO material is used for belts with density of 7850 kg/mm3. Loading and unloading function for the FE belts are specified. The contact between the dummy and the belt is defined by kinematic contacts with coefficient of friction of 0.3. The belt section of the shoulder belt is in contact with the right clavicle, the right upper arm, the neck and the collar, the left and right upper torso, the ribs, the sternum, breasts and the abdomen. The FE belt section of the lap belt is in contact with the hips, abdomen, the bottom ribs and the lower torso of the dummy. To run the analysis, MADYMO is coupled with LS-DYNA using the simple coupling and the analysis is run for 0.015 sec the maximum simulation time limit is 16ms [15]. Animation sequence is shown in figure 3.22.

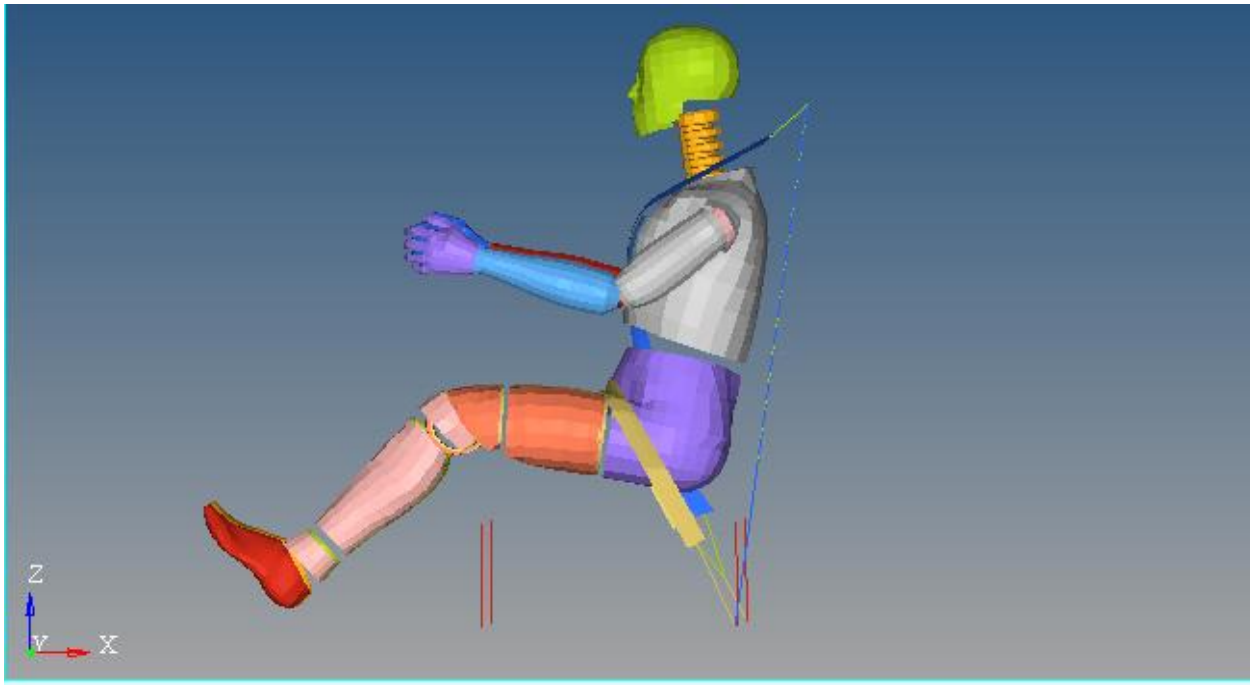

Figure 3.22. a, t = 0.000s

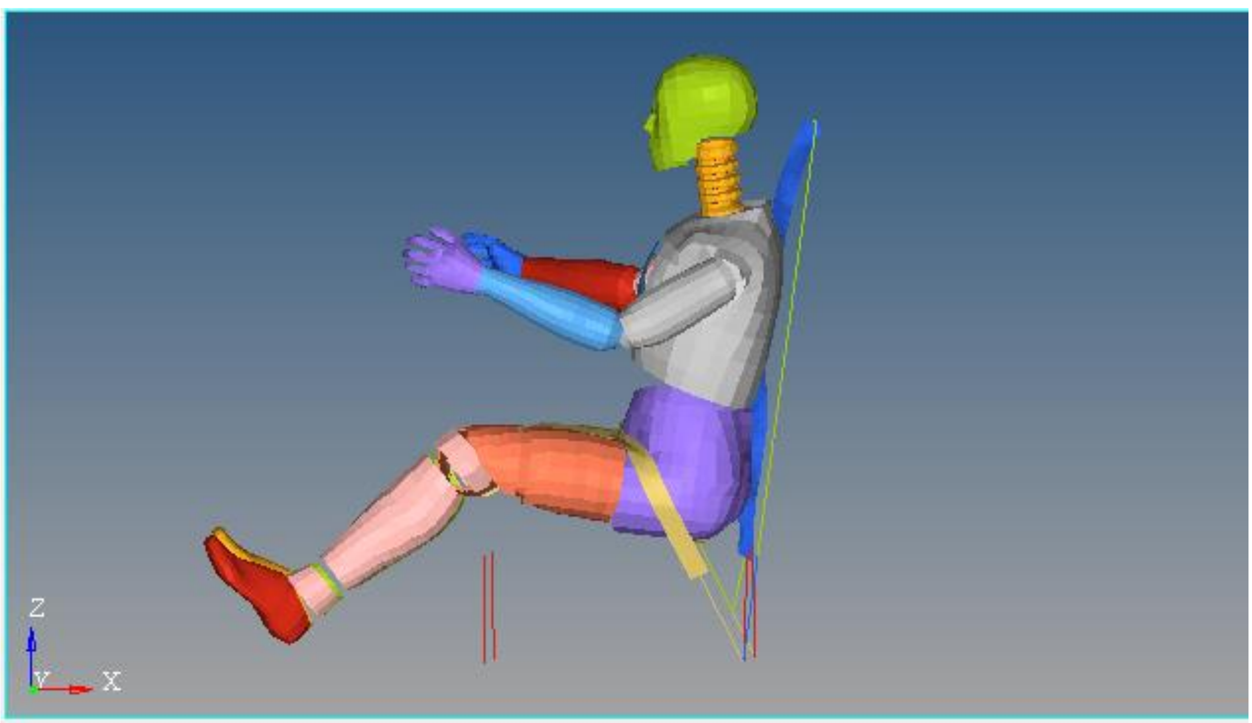

Figure 3.22. b, t = 0.0033s

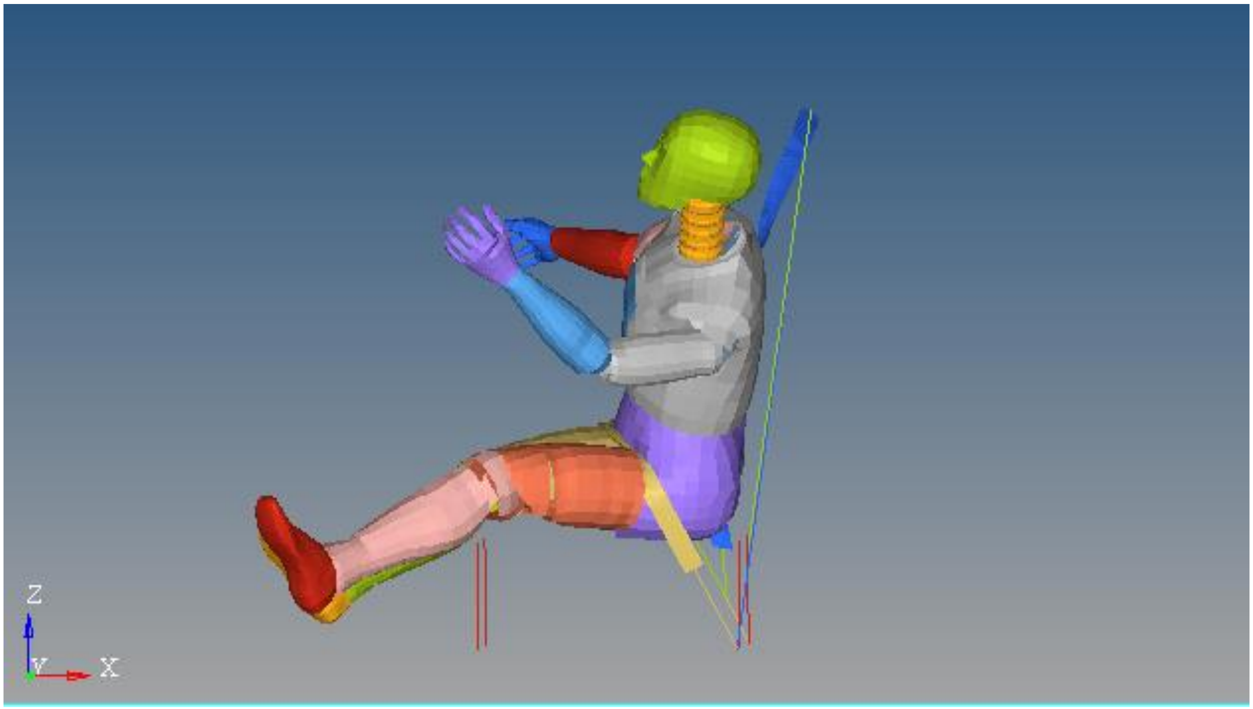

Figure 3.22. c, t = 0.009s

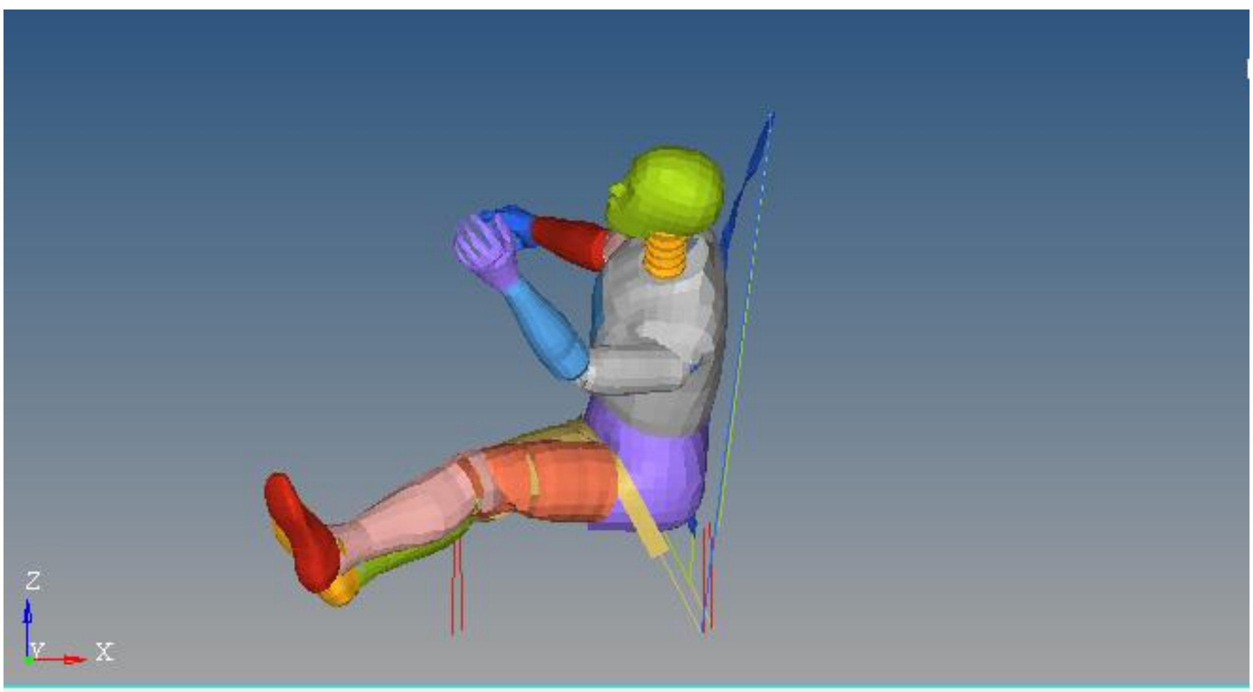

Figure 3.22. d, t = 0.015s

Figure 3.22. MADYMO dummy crash sequence

3.9.4. Potential injuries

The below graphs shows the comparison of Head CG acceleration of driver occupant for steel B-Pillar and composite B-Pillar, From the figure 3.23, it can be observed that the head CG acceleration for the car with composite fiber is lower as compared to the present steel B-pillar model. Acceleration for the steel B-Pillar is around 96 g's whereas the carbon fiber B-Pillar is around 21 g's. Due to this, the injury criteria HIC, reduces tremendously

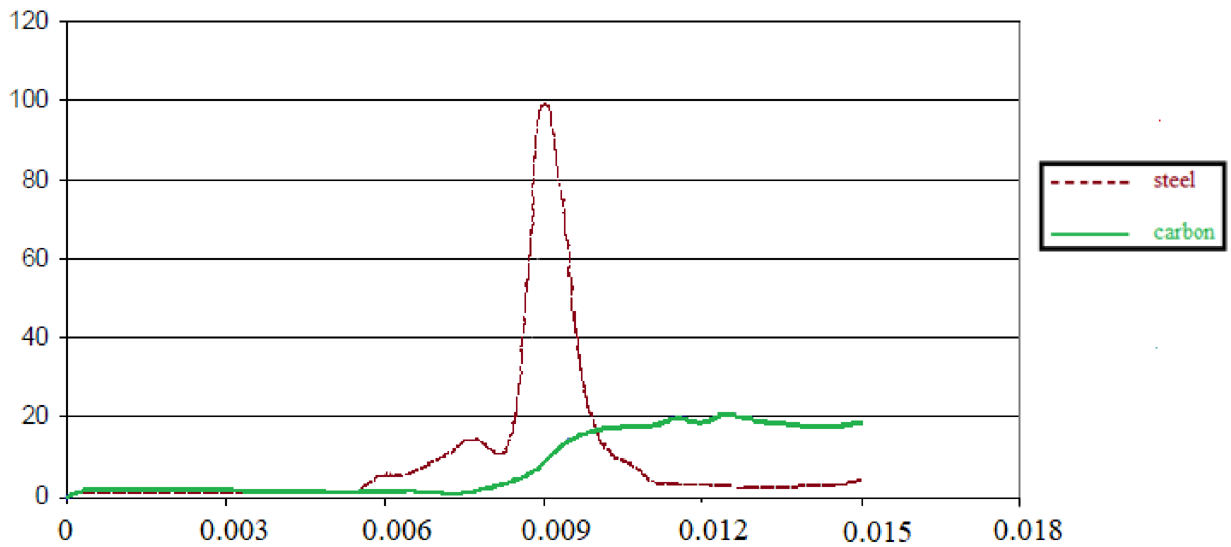

Figure 3.23. Head acceleration

Figure 3.24 shows the comparison of Thorax Spine acceleration of driver occupant for steel B-Pillar and composite B-Pillar. Carbon fiber exhibits lesser acceleration than the other impact B-Pillar. Acceleration of the present B-Pillar is around 37 g's and the new designed B-Pillar with carbon fiber is around 14 g's.

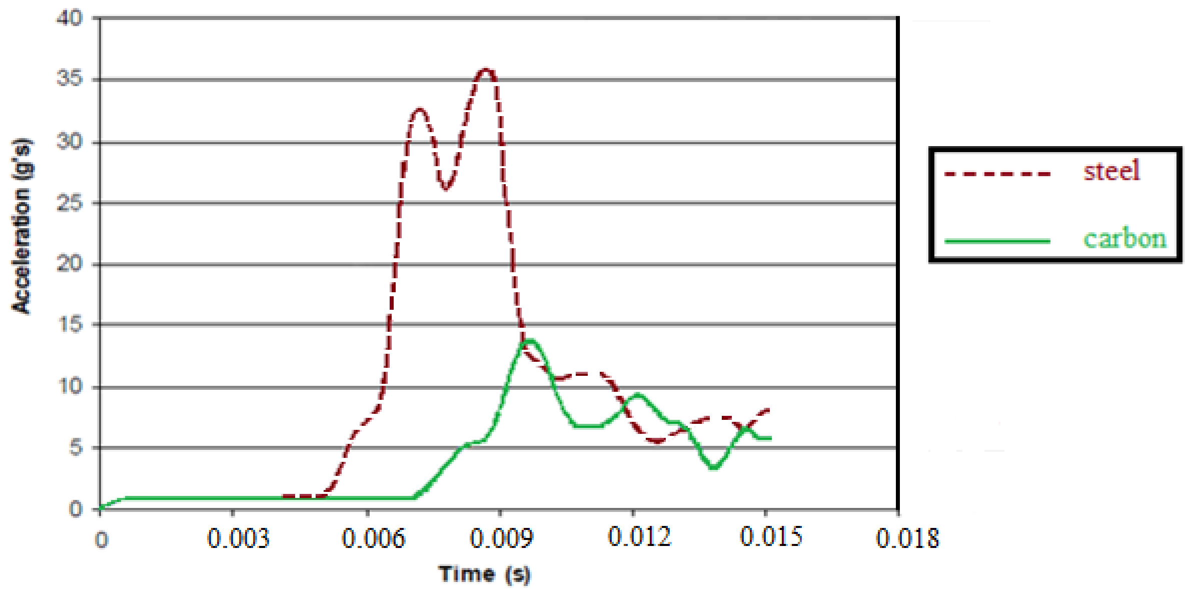

Figure 3.24. Thorax trauma index

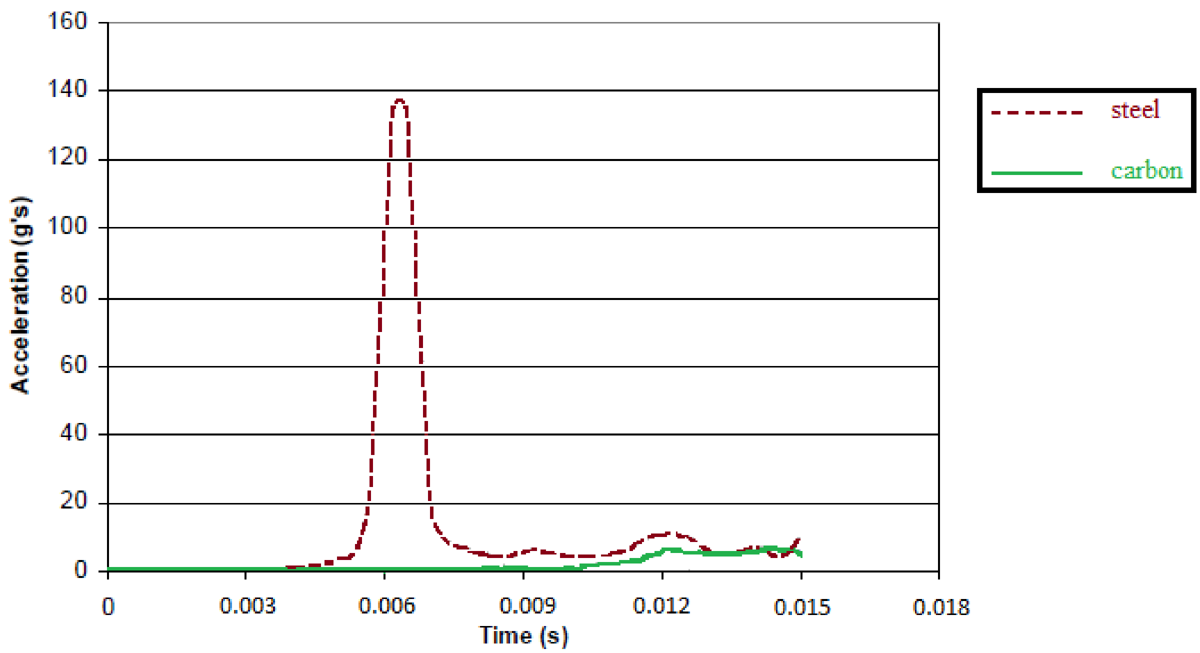

Figure 3.25. Pelvic acceleration

Figure 3.25 illustrates the curve between acceleration of pelvis regions. It can be seen that the composite fiber dominates in having lesser acceleration (5 g) than the steel (138 g) side impact B-

Pillar. This also indicates that the energy absorption of the composite fiber B-Pillar is higher and thus it helps in reducing injuries to the occupant.

Table 3.12. Injury rating (in g) [18]

Injury measure	Good	Acceptable	Marginal	Limit
HIC	0-623	624-779	780-985	>1000
V*C	0-1.00	1.01-1.20	1.21-1.3	>1.40
TTI	0-90	91-100	101-110	>120
Pa				>130

Table 3.13. Injury criteria (in g) calculated for the side impact crash

	Steel model	Carbon fiber model
HIC	973	263
Head CG acceleration	96	21
Thorax trauma index	40	15
Pelvis acceleration	138	5

Table 3.13 shows the injury rating standards according to Insurance Institute for Highway Safety. The head injury criteria and viscous injury criteria ratings are shown and we can see which is a good structure and a bad structure according to the values obtained. To supplement head injury measures, the movements and contacts of the dummies' heads during the crash are evaluated. This assessment is more important for seating positions without head protection airbags, which (assuming they perform as intended) should prevent injurious head contacts. Very high head injury measures typically are recorded when the pole hits the dummy head during impact.

CHAPTER FOUR

RESULT AND DESCUSSION

In this study ply thickness and orientation analysis of carbon fiber, internal energy of both steel and carbon fiber, deformation, velocity at which max deformation occurs and dummy injury criterion were discussed in the above chapter. In this chapter the results of both steel and carbon fiber are going to be discussed in comparison. Different cases of the analysis are collected, tabulated and compared in detail in each case and also remarks have been given. The remark is given to the carbon fiber pillar results status when compared to the steel pillar status as follow

4.1. Ply thickness and orientation selection for carbon fiber

As it is seen from the table below different orientations and thicknesses of the pillar were analyze for stress, strain, deformation and composite failure. A deformation of 10.07 mm is attained when the thickness is set to 1.6 mm. but when the thickness is set to 4.15 mm the deformation is 1.917 mm. which is less. Similarly the stress and strain values decrease when the thickness is increased from 1.6 mm to 4.15 mm.

When comparing the thickness t=2.9mm has 62.2 % less deformation than t=1.6 mm, and t=4.15 has 78.2 % less deformation than 1.6 mm. Therefore the thickness 4.15 mm is selected. After selecting the thickness the ply orientation was selected from

a. 0°,90°,45°,90°,0°
b. 0°,45°,0°,45°,0°,45°,0°,45°,0°
c. 0°,30°,-30°,60°,-60°,90°,0°,90°,-60°,60°,-30°,30°,0°

Even though the ply orientation showed relatively small differences; still ply orientation 0°,45°,0°,45°,0°,45°,0°,45°,0 °is selected because it has relatively better results of deformation, stress and strain when compared to the other orientations. The composite failure criterion is $1.25 + e^{-1}$ which less than 0 there is for it is safe according to fiber breakage failure criteria.

Table 4.1. Ply thickness and orientation summery

B-pillar thickness (mm)	Ply orientation	Ply thickness	Intrusion (mm)	v.stress (MPa)	v.strain (MPa)	Composite failure
1.6	A	0.32	9.828	59.32	$3.98 + e^{-3}$	$5.33 + e^{-1}$
	B	0.177	10.07	55.89	$3.99 + e^{-3}$	$6.4 + e^{-1}$
	C	0.13	8.79	56.63	$3.81 + e^{-3}$	$5.5 + e^{-1}$
2.9	A	0.58	3.332	34.12	$2.27 + e^{-3}$	$2.02 + e^{-1}$
	B	0.32	3.379	32.36	$2.16 + e^{-3}$	$2.24 + e^{-1}$
	C	0.22	3.396	34.84	$2.32 + e^{-3}$	$2.19 + e^{-1}$
4.15	A	0.832	1.953	24.51	$1.63 + e^{-3}$	$1.62 + e^{-1}$
	B	0.46	1.917	23.27	$1.54 + e^{-3}$	$1.25 + e^{-1}$
	C	0.32	1.945	24.78	$1.64 + e^{-3}$	$1.64 + e^{-1}$

4.2. Internal energy absorption, Deformation, velocity and weight of steel and carbon fiber

Internal energy of the material specifies the ability of the material to withstand the load while it is deformed. The B-pillar was impacted with a rigid pole 254 mm diameter according to Euro NCAP having Initial velocity of 29 Km/h. The analysis is run for 0.15 seconds and then the results are noted. The point of contact of the Impactor was according to the regulations. The analysis was done for both steel and carbon fiber , in this case carbon proved to be the best material as the energy absorption of carbon is twice as that of steel which is the original material. The internal energy of steel is $3.1 + e^7$J= 31 MJ where as carbon fiber has$6.25 + e^7 J = 62.5MJ$. This shows carbon fiber is 50.4 % better at absorbing energy than steel.

Table 4.2. Material Energy Absorption

Steel	31 MJ
Carbon Fiber	62.5 MJ

The carbon fiber pillar showed a deformation of 399.4 mm whereas steel pillar showed 579.7 mm. This shows carbon fiber 31.1 % less deformation than steel. The EuroNCAP experimental test has a deformation of 734 mm, therefor comparing results it is less. The velocity for which the maximum deformation occurs in the case of carbon fiber and steel B-pillars are 3.6m/s and 9.41 m/s respectively. This implies that steel pillar deforms on the time of impact where as carbon fiber pillar deforms slowly after impact.

Table 4.3. Deformation and velocity of materials for side impact crash

Material	Deformation (mm)	Velocity @ max deformation (m/s)
Steel	579.7	9.402
Composite	399.4	3.681

Total mass of the composite is 57.957% less when compared to the total mass of the steel B-pillar and absorb more deformational energy. Thickness of the composite B-pillar is of 4.15 mm in order to maintain the equivalent stiffness and energy absorption.

4.3. Dummy injury criterion

Hybrid III 50th percentile side impact dummy model was merged with the Ford Taurus vehicle. Here the seat belts were developed in MADYMO. Loading and unloading function for the FE belts were specified. The contact between the dummy and the belt was defined by kinematic contacts with coefficient of friction to be 0.3. The belt section of the shoulder belt is set in contact with the right clavicle, the right upper arm, the neck and the collar, the left and right upper torso, the ribs, the sternum, breasts and the abdomen. The FE belt section of the lap belt is in contact with the hips, abdomen, the bottom ribs and the lower torso of the dummy. To run the analysis, MADYMO is coupled with LS-DYNA using the simple coupling and the analysis is run for 0.015 sec.

Table 4.4. Injury criteria calculated for the side impact crash

	Steel model	Carbon fiber model
HIC	973	263
Head CG acceleration	86	22
Thorax trauma index	40	15
Pelvis acceleration	138	5

This analysis was done by validating by the injury rating standards according to Insurance Institute for Highway Safety. The head injury criteria and viscous injury criteria ratings are shown and we can see which is a good structure and a bad structure according to the values obtained. To supplement head injury measures, the movements and contacts of the dummies' heads during the crash are evaluated. This assessment is more important for seating positions without head protection airbags, which should prevent injurious head contacts. Very high head injury measures typically are recorded when the pole hits the dummy head during impact. Analysis of the movement and contact points of the dummies' heads during the Side impact crash test is used to assess this aspect of protection.

Table 4.4 shows the injury criteria calculated during a side impact crash test. For head injury criteria (HIC) a value of 623g is specified as the concussion tolerance level in side impacts. It can be seen that the Head CG Acceleration value for the carbon fiber is 263g which is very less when compared to steel with HIC of 973g and is very much accepted in the field of crashworthiness. This shows 72.9 % less than steel. Steel has HIC below the limit that is 1000g but still very critical that can cause high risk of death to the occupant.

The TTI is the acceleration criterion based on accelerations of the lower thoracic spine and the ribs. The TTI can be used as an indicator for the side impact performance of passenger cars. The dynamic performance requirement, as stated in Euro NCAP regulations, is that the TTI (d) level shall not exceed 85 g for passenger cars with four side doors and 90 g for two side doors. We can see that carbon fiber is about 15g's which is 62.5 % less than a steel pillar that is about 40g's. Both materials are very less than the specified standards.

The pelvic acceleration standard shows that a good structure is whose g-levels are less than 130 according to Euro NCAP Test Protocol. It can be seen that the pelvis acceleration levels are very less and are very much accepted in the field of crashworthiness. Carbon fiber pillar showed 96.5 % less cause of pelvic acceleration to the dummy.

CHAPTER FIVE

CONCLUSION AND RECOMMENDATION

5.1. Short summery

This research focuses on analyzing the crashworthiness of a vehicle B-pillar for occupant safety by using composite material instead of steel for the case of side impact in sedan car. The Finite Element model of existing Ford Taurus sedan car having steel B-pillar is used and analyzed in Hyper Mesh and LS-Dyna software's incorporated with MADYMO for crashworthiness. Then by changing the material in to composite material the Pillar was tested on different grounds to find out the maximum possible energy absorbing material, orientation and thickness. The two main aspects of crashworthiness which are intrusion and crash energy absorbing capacity of both materials are analyzed by crashing the vehicle in to rigid pole at a speed of 29 km/h according to EURONCAP test protocol. At the same time the head injury criteria's are analyzed for both materials to insure occupant safety according to IIHS. There for the steel B-pillar of the vehicle is modified by changing the material type to composite without changing the existing dimensions and then getting less deformation and greater crash energy absorbing capacity than the existing pillar which resulted in decrease in occupant injury.

5.2. Conclusion

In this thesis work steel and composite carbon fiber materials were analyzed for crashworthiness of Ford Taurus B-pillar in the case of side impact when vehicle is colliding with rigid pole. Ford Taurus is selected as a crash vehicle because it represents the small to mid-size sedan car to perform side crash analysis according to Euro NCAP Test Protocol. As a result the following conclusions are made

- When comparing the thickness of composite material from 1.6-4.15mm while setting the ply orientation to be 0°,45°,0°,45°,0°,45°,0°,45°,0°, the thickness 2.9mm has 62.2 % less deformation than t=1.6 mm, and t=4.15 has 78.2 % less deformation than 1.6 mm.
- The internal energy of carbon fiber is 50.4 % better at absorbing energy than steel.

- The carbon fiber pillar showed a deformation of 399.4 mm whereas steel pillar showed 579.7 mm. This shows carbon fiber 31.1 % less deformation than steel.
- The velocity for which the deformation occurs in the case of carbon fiber and steel B-pillars are 3.6m/s and 9.41 m/s respectively which implies that steel pillar deforms on the time of impact where as carbon fiber pillar deforms slowly after impact which highly decreases the possibility of fatality during the impact.
- It can be seen that the Head acceleration value for the carbon fiber is 263g's which is very less when compared to steel with HIC of 973g's which shows 72.9 % less HIC than steel.
- It can be seen that the TTI of the dummy in a carbon fiber pillar vehicle is about 15g's which is 62.5 % less than a steel pillar that is about 40g's.
- Carbon fiber pillar also showed 94.5 % less cause of pelvic acceleration to the dummy than steel.
- Total mass of the composite is 57.957% less when compared to the total mass of the steel B-pillar and absorb more deformational energy.

5.3. Recommendation for future work

This study is initiated to decrease the occupant fatality caused due to side crash in our country. Therefore detailed strength analysis and design optimization of the B-pillar and other structures of the vehicle is to be analyzed using different software's.

The model has the potential to decrease the injury due to the head colliding to the B-pillar of the vehicle. But detailed on the side beam, door and roof of the vehicle should also be done to minimize all kinds of injury to the occupant.

Experimental tests should also be studied for the different crash types of the vehicle. Since vehicle manufacturing is a new technology in Ethiopia it is highly recommended to test the vehicles for crashworthiness before supplying to costumers.

Finally side air bag is highly recommended to minimize the fatal rate due to side crash.

REFERENCE

1. Ms. Gauri B. Mahajan1 and Prof. Dinesh. N. Kamble, (2015), “Crash and Impact Strength Analysis of Structural component of the vehicle for Occupant Safety”, International Journal of Science, Engineering and Technology Research (IJSETR), Volume 4, Issue 12,
2. S. Venkata Krishna, Vinod K. Banthia, (2005), “Reduction in Intrusion of B-Pillar in Side Impact using Advanced High Strength Steel Components”, Faculty of Engineering and Technology, M. S. Ramaiah University of Applied Sciences, Bangalore 560 054.
3. State of Florida Author’s Guide (2006) Crashworthiness and Impact Analysis Laboratory “Crash and Safety Testing Standard for Para transit Buses Acquired by The State of Florida”, FAMU-FSU College of Engineering, FL 32310-6046
4. Wang Dazhi, DONG Guang., (2006), “Car Side Structure Crashworthiness in Pole and Moving Deformable Barrier Side Impacts”, Tsinghua Science and Technology, ISSN 1007-0214 13/15 pp725-730, Volume 11, Number 6.
5. Marklund and L. Nilsson, (2001), “Optimization of a car body component subjected to side impact”, Industrial applications and case studies Struct Multidisc Optim 21, 383–392 Springer Verlag.
6. Aniekan Essienubong Ikpe and Ejiroghene Kelly Orhorhoro, (2017), “Design and Reinforcement of a B-Pillar for Occupants Safety in Conventional Vehicle Applications”, International Journal of Mathematical, Engineering and Management Sciences, Vol. 2, No. 1, 37–52, 2017 ISSN: 2455-7749 37.
7. Getu S. Tulua, (2013), “Characteristics of Police-reported Road Traffic Crashes in Ethiopia over a Six Year Period", Simon Washington Centre for Accident Research and Road Safety – Queensland (CARRS-Q), Queensland University of Technology Corresponding.
8. Philipps, M., Patberg, L., (1998), “Structural Analysis and Testing of Composites in Automotive Crashworthiness Application”, SAE Special Publications, Safety and Material Test Methodologies, v 1320, pp. 97-101.
9. Jacob, C.G., Fellers, F.J., (1996), "Energy Absorption in Polymer Composites for Automotive Crashworthiness".

10. Fleming, D.C., (1991), “The Energy Absorption of Graphite/Epoxy Truncated Cones,” M.S. Thesis, Department of Aerospace Engineering, University of Maryland, College Park.
11. R Adam, H., Patberg, L., Philipps, (1998), “Testing of New Composite Side Door Concepts”, Proceedings of the 1998 SAE International Congress & Exposition, SAE Special Publications, Vol. 1320, pp. 23-30.
12. Federal Motor Vehicle Safety Standards (FMVSS), (1995), “Side Impact Protection. U.S Department of Transportation”. No.214.
13. MADYMO User Manual Version, 6.0.1.
14. Imtiaz Shareef Gandikota, (2006), “Multilevel design optimization of automotive structures using dummy- and vehicle-based responses”.
15. European New Car Assessment Program (Euro NCAP), (2011), “Pole Side Impact Testing Protocol”, Version 5.2.
16. Yao-Jun Zheng, (2009), “Vehicle Side Crash Safety Research based on Dynamics Modeling and Analysis”, Zhejiang Technical Institute of Economics, Hang Zhou, Zhejiang, 310018, China.
17. Adrian Fails and Roy Minton, (2011), “Comparison of EuroNCAP Assessments with Injury Causation in Accidents”, TRL Limited United Kingdom Document, Number 319.
18. IIHS, (2017) “Side Impact Crashworthiness Evaluation Crash Test Protocol”, (Version X),
19. Dinesh Ugale, Rajiv Gandhi, (2013), "Effective Dynamic Side Impact (DSI) Beam Design for IIHS Side Pole Impact Using RADIOSS”, Tata Technologies Ltd 25, Pune – 411 057, India.
20. LS-Dyna User's Manual, Version 970.
21. Hyper Mesh User Manual, Version 10.1.
22. Beruk Hailu, T. Ashokkumar, (2000), “A New Accident Proof Material Design for B - Pillar of A Car”, Institute of Technology, Haramya University, Dire Dawa, Ethiopia.
23. Harijono Djojodihardjo and Soo Lin Khai, (2013) “Modeling, Analysis and Comparative Study of Side Impact Beam”, International Journal of Engineering and Innovative Technology (IJEIT),

24. Brock Watson, Brett Campbell, Duane Cronin, (2001), “study of vehicle dynamics and occupant response in side impact crash tests”, University of Waterloo Canada, Paper Number 09-0016.
25. Mr. C.Venkataswamy, Mr. T.Naganna, Mr. Nirmith Kumar Mishra, (2015), “Modeling And Analysis Of B-Pillar”, International Journal of Advanced Engineering and Global Technology, Vol-03, Issue-08.
26. Hampton C. Gabler, Brian N, (2005), “Side Impact Injury Risk for Belted Far Side Passenger Vehicle Occupants”, Fildes Monash University, Accident Research Centre Laurie Sparke Holden Innovation, 01-0287
27. Hideki Yonezawa, Naruyuki Hosokawa, (2003), “Investigation for New Side Impact Test Procedures in Japan”, National Traffic Safety and Environment Laboratory Nagoya University, Japan, Paper Number 09-0369
28. Sushrut Joglekar, B. D. Patil, Bavdhan, (2017), “Vibration Analysis of Composite Reinforced B- Pillar used in Automobiles”, Bavdhan, Pune, Maharashtra, India, Vol. 6, Issue 7
29. Guangyao Zhao, Yifeng Zhao, Xuejiao Li, (2012), “Whole Car Side Impact Mode and Response Evaluation”.
30. L.J. Sparke, J.A. Tomas., (2006), “Crash Pulse Optimization for Minimum Injuring Risk to Car Occupants”, J SAE Paper 2006, No.09-0712.
31. Douglas J Stein., (2006), “Apparatus and Method for Side Impact Testing”, J. SAE, paper NO.970 575
32. Iyengar R.M., Fedewa B., (2008), “Implications of Hot-Stamped Boron Steel Components in Automotive Structures”, SAE Technical Paper Series.
33. Strother C E, Kent R W, Warner C Y. (2000) “Estimating vehicle deformation energy for vehicle struck in the side”. SAE paper number 980215.
34. Ruan J S, Khalil T, King A I., (1999), “Human head dynamic response to side impact by finite element modeling. Journal of Biomechanical Engineering”, 113(3), 276-283.
35. Farmer C M, Braver E R, Mitter E L., (1997), “Two-vehicle side impact crashes: The relationship of vehicle and crash characteristic to injury severity”, Accident Analysis & Prevention, 29(3) 399-406.

APPENDIX I

EUROPEAN NEW CAR ASSESSMENT PROGRAMME (Euro NCAP)

ASSESSMENT PROTOCOL – ADULT OCCUPANT PROTECTION

1. INTRODUCTION

Euro NCAP's original assessment protocol was developed jointly by TRL and Vehicle Safety Consultants Ltd under contract to the UK Department of the Environment Transport and the Regions and International Testing, respectively. Subsequent versions of the protocol have been developed and released by the Euro NCAP Secretariat. Beginning with Version 5 important changes have been included that have been brought about by the introduction of the overall rating scheme. Individual documents are released for the four main areas of assessment:

- Assessment Protocol – Adult Occupant Protection;
- Assessment Protocol – Child Occupant Protection;
- Assessment Protocol – Pedestrian Occupant Protection;
- Assessment Protocol – Safety Assist;

In addition to these four assessment protocols, a separate document is provided describing the method and criteria by which the overall safety rating is calculated on the basis of the car performance in each of the above areas of assessment.

The following protocol deals with the assessments made in the area of Adult Occupant Protection, in particular in the frontal offset deformable and full width impact tests, the side impact barrier test, the pole test and the whiplash tests.

DISCLAIMER:

Euro NCAP has taken all reasonable care to ensure that the information published in this protocol is accurate and reflects the technical decisions taken by the organization. In the unlikely event that this protocol contains a typographical error or any other inaccuracy, Euro NCAP reserves the right to make corrections and determine the assessment and subsequent result of the affected requirement(s).

2. METHOD OF ASSESSMENT

The starting point for the assessment of adult occupant protection is the dummy response data recorded in five different test configurations: frontal impact in offset and full overlap, side impact, pole impact and (low speed) rear impact. All criteria used are calculated according to Technical Bulletin 17. Initially, each relevant body area is given a score based on the measured dummy parameters. These scores can be adjusted after the test based on supplementary requirements. E.g. for frontal impact, consideration is given to whether the original score should be adjusted to reflect occupant kinematics or sensitivity to small changes in contact location, which might influence the protection of different sized occupants in different seating positions. The assessment also considers the structural performance of the car by taking account of such aspects as steering wheel displacement, pedal movement, foot well distortion and displacement of the A pillar. The adjustments (or modifiers) based on both inspection and geometrical considerations are applied to the body area assessments to which they are most relevant.

For frontal offset impact, the score for each body area is based on the driver data, unless part of the passenger fared less well. It is stated that the judgment relates primarily to the driver. For frontal full width, the score is based on driver and rear passenger. Side impact and pole impact results relate to the struck-side occupant only, while Whiplash results cover front and rear occupants. No attempt is made to rate the risk of life threatening injury any differently from the risk of disabling injury. Similarly, no attempt is made to rate the risk of the more serious but less frequent injury any differently from the risk of less serious but more frequent injury. Care has been taken to try to avoid encouraging manufacturers from concentrating their attention on areas which would provide little benefit in accidents.

From the information collected in the five test scenarios, individual test scores are computed for the frontal tests, side and pole impact and whiplash protection. The adjusted score for the different body regions is presented, in a visual format of coloured segments within a human body outline. This is presented for the driver and front/rear seat passenger in frontal impact, for the driver in side and pole impact and for all occupants in rear impact. Finally, for the complete area of adult occupant protection assessment, the scores for frontal, side, pole and whiplash are summed. The resulting Adult Occupant Protection Score is expressed as a percentage of the maximum achievable number of points.

In addition to the basic Euro NCAP assessment, additional information is recorded and may be reported. In future, some of these additional aspects may be added to the Euro NCAP assessment

2.1. Points Calculation

From Phase 3, a sliding scale system of points scoring has been used to calculate points for each measured criterion. This involves two limits for each parameter, a more demanding limit (higher performance), below which a maximum score is obtained and a less demanding limit (lower performance), beyond which no points are scored. In frontal, side, and pole impacts, the maximum score for each body region is four points; for rear impact protection, it is three points*. Where a value falls between the two limits, the score is calculated by linear interpolation.

Capping

Capping limits are maintained for criteria related to critical body regions. Exceeding a capping limit generally indicates unacceptable high risk at injury or, in the case of the whiplash tests, an unacceptably high seat design parameter. In all cases, this leads to loss of all points related to the tests. Capping limits can be equal to or higher than the lower performance limit, depending on the test.

3. OFFSET DEFORMABLE BARRIER FRONTAL IMPACT ASSESSMENT

3.1. Criteria and Limit Values

The basic assessment criteria used for frontal impact, with the upper and lower performance limits for each parameter, are summarized below. Where multiple criteria exist for an individual body region, the lowest scoring parameter is used to determine the performance of that region. The lowest scoring body region of driver or passenger is used to determine the score. For the frontal offset deformable barrier impact, capping is applied on the critical body regions: head, neck and chest.

Head

Drivers with Steering Wheel Airbags and Passengers

If a steering wheel airbag is fitted the following criteria are used to assess the protection of the head for the driver. These criteria are always used for the passenger.

Note:

HIC15 levels above 1000 have been recorded with airbags, where there is no hard contact and no established risk of internal head injury. A hard contact is assumed if the peak resultant head acceleration exceeds 80g or if there is other evidence of hard contact. If there is no hard contact a score of 4 points is awarded. If there is hard contact, the following limits are used:

Higher performance limit		
HIC_{15}	500	
Resultant Acc. 3 msec exceedence	72g	
Lower performance and capping limit		
HIC_{15}	700	(20% risk of injury AIS3 [1,2])
Resultant Acc. 3 msec exceedence	80g	

Drivers with No Steering Wheel Airbag

If no steering wheel airbag is fitted, and the following requirements are met in the frontal impact test:

HIC_{15} <700

Resultant Acc. 3 msec exceedence <80g,

Then 6.8 kg spherical head form test specified in ECE Regulation 12 [3] are carried out on the steering wheel. The tester attempts to choose the most aggressive sites to test and it is expected that two tests will be required, one aimed at the hub and spoke junction and one at the rim and spoke junction. The assessment is then based on the following criteria:

Higher performance limit

Resultant peak Acc.	80g
Resultant Acc. 3 msec exceedence	65g

Lower performance and capping limit

HIC_{15}	700
Resultant peak Acc.	120g
Resultant Acc. 3 msec exceedence	80g

From the face form tests, a maximum of 2 points are awarded for performance better than the lower limits. For values worse than the lower performance limit, no points are awarded.

The results from the worst performing test are used for the assessment. This means that for cars, not equipped with a steering wheel airbag, the maximum score obtainable for the driver's head is 2 points.

Neck

Higher performance limit

Shear	1.9kN @ 0 msec,	1.2kN @ 25 - 35msec,	1.1kN @ 45msec
Tension	2.7kN @ 0 msec,	2.3kN @ 35msec,	1.1kN @ 60msec
Extension	42Nm		

Lower performance and capping limit

Shear	3.1kN @ 0msec,	1.5kN @ 25 - 35msec,	1.1kN @ 45msec*
Tension	3.3kN @ 0msec,	2.9kN @ 35msec,	1.1kN @ 60msec*
Extension	57Nm*	(Significant risk of injury [4])	

Note: Neck Shear and Tension are assessed from cumulative exceedence plots, with the limits being functions of time. By interpolation, a plot of points against time is computed. The minimum point on this plot gives the score.

Chest

Higher performance limit

Compression 22mm (5% risk of injury AIS3 [5])

Viscous Criterion 0.5m/sec (5% risk of injury AIS4) *Lower performance and capping limit*

Compression	42mm	
Viscous Criterion	1.0m/sec	(25% risk of injury AIS4)

Knee, Femur and Pelvis

Higher performance limit

Femur compression	3.8kN	(5% risk of pelvis injury [6])
Knee slider compressive displacement	6mm	

Lower performance limit

Femur Compression	9.07kN @ 0msec,	
	7.56kN @ 10msec*	(Femur fracture limit [4])
Knee slider compressive displacement	15mm* (Cruciate ligament failure limit [4,7])	

Note:

Femur compression is assessed from a cumulative exceedence plot, with the limits being functions of time. By interpolation, a plot of points against time is computed. The minimum point on this plot gives the score. The Lumbar forces and moments are measured for monitoring purpose only.

Lower Leg

Higher performance limit

Tibia Index	0.4
Tibia Compression	2kN

Lower performance limit

Tibia Index	1.3*

Tibia Compression	8kN*	(10% risk of fracture [4,8])

Foot/Ankle

Higher performance limit

Pedal rearward displacement 100mm

Lower performance limit

Pedal rearward displacement 200mm

Notes:

- Pedal displacement is measured for all pedals with no load applied to them.
- If any of the pedals are designed to completely release from their mountings during the impact, no account is taken of the pedal displacement provided that release occurred in the test and that the pedal retains no significant resistance to movement.
- If a mechanism is present to move the pedal forwards in an impact, the resulting position of the pedal is used in the assessment.
- The passenger's foot/ankle protection is not currently assessed.

3.2. Modifiers

Driver

The score generated from driver dummy data may be modified where the protection for different sized occupants or occupants in different seating positions, or accidents of slightly different severity, can be expected to be worse than that indicated by the dummy readings or deformation data alone. There is no limit to the number of modifiers that can be applied. The concepts behind the modifiers are explained in Section 8.

Head

Unstable Contact on the Airbag

If during the forward movement of the head its center of gravity moves further than the outside edge of the airbag, head contact is deemed to be unstable. The score is reduced by one point. If for any other reason head protection by the airbag is compromised, such as by detachment of the steering wheel from the column, or bottoming-out of the airbag by the dummy head, the modifier is also applied.

Note:

Head bottoming-out is defined as follows: There is a definite rapid increase in the slope of one or more of the head acceleration traces, at a time when the dummy head is deep within the airbag. The acceleration spike associated with the bottoming out should last for more than 3ms.The acceleration spike associated with the bottoming out should generate a peak value more than 5 g above the likely level to have been reached if the spike had not occurred. This level will be established by smooth extrapolation of the curve between the start and end of the bottoming out spike.

Hazardous Airbag Deployment

If, within the head zone, the airbag unfolds in a manner in which a flap develops, which sweeps across the face of an occupant vertically or horizontally the -1 point modifier for unstable airbag contact will be applied to the head score. If the airbag material deploys rearward, within the "head zone" at more than 90 m/s, the -1 point modifier will be applied to the head score. Further details are contained in Euro NCAP Technical Bulletin TB 001.

Incorrect Airbag Deployment

Any airbag(s) which does not deploy fully in the designed manner will attract a -1 point modifier applicable to each of the most relevant body part(s) for the affected occupant. For example, where a steering wheel mounted airbag is deemed to have deployed incorrectly, the penalty will be applied to the frontal impact driver's head (-1). Where, a passenger knee airbag fails to deploy correctly, the penalty will be applied to the frontal impact passenger left and right knee, femur and pelvis (1).

Where the incorrect deployment affects multiple body parts, the modifier will be applied to each individual body part. For example, where a seat or door mounted side airbag, that is intended to provide protection to the head as well as the thorax, abdomen or pelvis deploys incorrectly, the penalty will be applied to two body regions, -1 to the head and -1 to the chest.

The modifier(s) will be applied to the scores of the impacts for which the airbag was intended to offer protection, regardless of the impact in which it deployed incorrectly. For example, the penalty will be applied to the side and pole impact scores if a side protection airbag deploys incorrectly during the frontal crash. Or, if a knee airbag deploys incorrectly in the full width impact, the modifier will be applied to the pelvic region of both the offset and full width tests. Where any frontal protection airbag deploys incorrectly, Euro NCAP will not accept knee mapping data for that occupant.

Unstable Contact on a Steering Wheel without an Air Bag

If, during the forward movement of the head, its center of gravity moves radially outwards further than the outside edge of the steering wheel rim, head contact is deemed to be unstable. The score is reduced by one point. If for any other reason head contact on the steering wheel is unstable, such as detachment of the steering wheel from the column, the modifier is also applied.

Displacement of the Steering Column

The score is reduced for excessive rearward, lateral or upward static displacement of the top end of the steering column. Up to 90 percent of the EEVC limits, there is no penalty. Beyond 110 percent of the EEVC limits, there is a penalty of one point. Between these limits, the penalty is generated by linear interpolation. The EEVC recommended limits are: 100mm rearwards, 80mm upwards and 100mm lateral movement. The modifier used in the assessment is based on the worst of the rearward, lateral and upward penalties.

Chest

Displacement of the A Pillar

The score is reduced for excessive rearward displacement of the driver's front door pillar, at a height of 100mm below the lowest level of the side window aperture. Up to 100mm displacement there is no penalty. Above 200mm there is a penalty of two points. Between these limits, the penalty is generated by linear interpolation.

Integrity of the Passenger Compartment

Where the structural integrity of the passenger compartment is deemed to have been compromised, a penalty of one point is applied. The loss of structural integrity may be indicated by characteristics such as:

- Door latch or hinge failure, unless the door is adequately retained by the door frame.
- Buckling or other failure of the door resulting in severe loss of fore/aft compressive strength.
- Separation or near separation of the cross facia rail to A pillar joint.
- Severe loss of strength of the door aperture.

When this modifier is applied, Euro NCAP will not accept knee mapping data.

Steering Wheel Contact

Where there is obvious direct loading of the chest from the steering wheel, a one point penalty is applied.

Shoulder belt load (Driver and Front Passenger)

Where the shoulder belt load measured, exceeds 6kN a two point penalty is applied.

Knee, Femur & Pelvis

Variable Contact

The position of the dummy's knees is specified by the test protocol. Consequently, their point of contact on the facia is pre-determined. This is not the case with human drivers, who may have their knees in a variety of positions prior to impact. Different sized occupants and those seated in different positions may also have different knee contact locations on the facia and their knees may penetrate into the facia to a greater extent. In order to take some account of this, a larger area of potential knee contact is considered. If contact at other points, within this greater area, would be more aggressive penalties are applied.

The area considered extends vertically 50mm above and below the maximum height of the actual knee impact location [8]. Vertically upwards, consideration is given to the region up to 50mm above the maximum height of knee contact in the test. If the steering column has risen during the test it may be repositioned to its lowest setting if possible. Horizontally, for the outboard leg, it extends from the center of the steering column to the end of the facia. For the inboard leg, it extends from the center of the steering column the same distance inboard, unless knee contact would be prevented by some structure such as a center console. Over the whole area, an additional penetration depth of 20mm is considered, beyond that identified as the maximum knee penetration in the test. The region considered for each knee is generated independently. Where, over these areas and this depth, femur loads greater than 3.8kN and/or knee slider displacements greater than 6mm would be expected, a one point penalty is applied to the relevant leg.

Concentrated Loading

The biomechanical tests which provided the injury tolerance data were carried out using a padded Impactor which spread the load over the knee. Where there are structures in the knee impact area which could concentrate forces on part of the knee a one point penalty is applied to the relevant leg.

Where a manufacturer is able to show, by means of acceptable test data, that the Variable Contact and/or Concentrated Loading modifiers should not be applied, the penalties may be removed.

If the Concentrated load modifier is not applied to either of the driver's knees, the left and right knee zones (defined above) will both be split into two further areas, a ‘column’ area and the rest of the facia. The column area for each knee will extend 60mm from the centerline of the steering column and the remainder of the facia will form the other area for each knee. As a result, the one point penalty for Variable Contact will be divided into two with one half of a point being applied to the column area and one half of a point to the remainder of the facia for each knee.

Lower Leg

Upward Displacement of the Worst Performing Pedal

The score is reduced for excessive upward static displacement of the pedals. Up to 90 percent of the limit considered by EEVC, there is no penalty. Beyond 110 percent of the limit, there is a penalty of one point. Between these limits, the penalty is generated by linear interpolation. The limit agreed by EEVC was 80mm.

Foot & Ankle

Foot well Rupture

The score is reduced if there is significant rupture of the foot well area. This is usually due to separation of spot welded seams. A one point penalty is applied for foot well rupture. The foot well rupture may either pose a direct threat to the driver's feet or be sufficiently extensive to threaten the stability of foot well response. When this modifier is applied, Euro NCAP will not accept knee mapping data.

Pedal Blocking

Where the rearward displacement of a 'blocked' pedal exceeds 175mm relative to the pre-test measurement, a one point penalty is applied to the driver's foot and ankle assessment. A pedal is blocked when the forward movement of the intruded pedal under a load of 200N is <25mm. Between 50mm and 175mm of rearward displacement the penalty is calculated using a sliding scale between 0 to 1 points.

Passenger

The score generated from passenger dummy data may be modified where the protection for different sized occupants or occupants in different seating positions, or accidents of slightly different severity, can be expected to be worse than that indicated by the dummy readings alone. There is no limit to the number of modifiers that can be applied. The concepts behind the modifiers are explained in section 7. The modifiers applicable to the passenger are:

- Unstable Contact on the airbag

- Hazardous airbag deployment
- Shoulder belt load
- Incorrect airbag deployment
- Knee, Femur & Pelvis, Variable Contact
- Knee, Femur & Pelvis, Concentrated loading

The assessments airbag stability, head bottoming-out (where present) and the knee impact areas are the same as for driver. For the outboard knee, the lateral range of the knee impact area extends from the center line of the passenger seat to the outboard end of the facia. For the inboard knee, the area extends the same distance inboard of the seat center line, unless knee contact is prevented by the presence of some structure such as the center console. The passenger knee zones and penalties will not be divided into two areas even if the concentrated load modifier is not applied.

Door Opening during the Impact

When a door opens in the test, a minus one-point modifier will be applied to the score for that test. The modifier will be applied to the frontal impact assessment for every door (including tailgates and moveable roofs) that opens. The number of door opening modifiers that can be applied to the vehicle score is not limited.

Door Opening Forces after the Impact

The force required to unlatch and open each side door to an angle of 45 degrees is measured after the impact. A record is also made of any doors which unlatch or open in the impact. Currently, this information is not used in the assessment but it may be referred to in the text of the published reports.

Door opening forces are categorized as follows:

Opens normally	Normal hand force is sufficient
Limited force	100N
Moderate force	> 100N to < 500N
Extreme hand force	500N
Tools had to be used	Tools necessary

3.3. Scoring & Visualization

The protection provided for adults for each body region are presented visually, using colored segments within body outlines. The color used is based on the points awarded for that body region (rounded to three decimal places), as follows:

Green	'Good'	4.000 points
Yellow	'Adequate'	2.670 - 3.999 points
Orange	'Marginal'	1.330 - 2.669 points
Brown	'Weak'	0.001 - 1.329 points
Red	'Poor'	0.000 points

For frontal impact, the body regions are grouped together, with the score for the grouped body region being that of the worst performing region or limb. The grouped regions are: Head and Neck (4 points), Chest (4 points), Knee, Femur, Pelvis (i.e. left and right femur and knee slider) (4 points) and Leg and Foot (i.e. left and right lower leg and foot and ankle) (4 points). Results are shown separately for driver and passenger.

The contribution of the frontal impact test to the Adult Occupant Protection Score is calculated by summing the body scores for the relevant body regions, taking the lower of the driver and passenger scores for each region (16 points total). This score is halved with a total achievable score of 8 points.

4. SIDE BARRIER AND POLE IMPACT ASSESSMENT

4.1. Criteria and Limit Values

The basic assessment criteria used for both side barrier and pole impacts, with the upper and lower performance limits for each parameter, are summarized below. The assessments are divided into four individual body regions, the head, chest, abdomen and pelvis. The criteria and limits are equal for side barrier and pole test except for the head and chest. A maximum of four points are available for each body region. Where multiple criteria exist for an individual body region, the lowest scoring parameter is used to determine the performance of that region. There is no limit to the number of modifiers that can be applied.

For both side and pole impacts, capping is applied on the head, chest, abdomen and pelvis. Where no head protection systems are present, the pole test will not be allowed and the points for that test are set to zero.

Note:

The requirement is for the fitment of a head protection system, meaning that the manufacturer is free to use a solution other than an airbag. However, for technologies other than conventional curtain or head airbags, the manufacturer is requested to provide evidence that the system is effective, at least in principle, before a test can be allowed.

Head

Side impact

Higher performance limit

HIC_{15}	500	
Resultant Acc. 3 msec exceedence	72g	
Lower performance and capping limit		
HIC_{15}	700	(20% risk of injury $\geq$ AIS3 [1,2])
Resultant Acc. 3 msec exceedence	80g	

Pole impact

Capping limits

HIC_{15}	<700
Peak Resultant Acc	<80g

No direct head contact with the pole

Chest

The assessment is based on the worst performing individual rib lateral compression.

MDB and Pole Higher performance limit

Lateral Compression 28mm (5% risk of AIS3, 67YO)

MDB Lower performance and capping limit		
Lateral Compression	50mm	(30% risk of AIS3, 45YO)
Pole Lower performance limit		
Lateral Compression	50mm	(30% risk of AIS3, 45YO)
Pole Capping limit		
Lateral Compression	**55mm**	**(50% risk of AIS3, 45YO)**
Abdomen		
Higher performance limit		
Lateral Compression	47mm	(33% risk of AIS3, 67YO)
Lower performance and capping limit		
Lateral Compression	65mm	
Pelvis		
Higher performance limit		
Pubic Symphysis Force	1.7kN	(5% risk of AIS3, 67YO)
Lower performance and capping limit		
Pubic Symphysis Force	2.8kN	(20% risk of AIS3, 45YO)

4.2. Modifiers

Shoulder

Where the shoulder lateral force (Y direction) component is 3.0kN or above, no points will be awarded for the chest assessment.

Chest & Abdomen

Where the viscous criterion (V*C) is 1.0m/s or above for the chest, abdomen or both, no points will be awarded for the relevant body region assessment.

Side Head Protection Device (Pole Impact Only)

Vehicles equipped with head protection side airbags, curtain, seat mounted or any other, will have the inflated energy absorbing areas evaluated by means of a geometric assessment. The airbags must provide protection for a range of occupant sizes in both the front and the rear on both sides of the vehicle. Where a vehicle does not offer sufficient protection, a penalty of -4 points, -2 for front and -2 for rear seats, shall be applied to the overall pole impact score. Any vehicle that does not provide a head protection device covering the front and rear seat positions on both sides of the vehicle will also attract this modifier.

Coverage areas

To ensure adequate head protection is offered, the head protection device coverage is assessed in the geometric area, or the Head Protection Device (HPD) assessment zone, where the occupant head would most likely impact side structures. If the vehicle is equipped with movable rear seats the seat shall be set to the most rearward position. If there is a third row of fixed seats, these will be included in the assessment unless they are per manufacturers' recommendation not suitable for adult occupation (handbook).

Application

Where the airbags differ between the left and right hand sides of the vehicle, the airbags on both sides of the vehicle will be evaluated and the assessment will be based upon worst performing side. All areas of the airbag, both front and rear, will be evaluated and the assessment will be based upon the worst performing part of any of the airbags.

Exclusions

The head protecting airbags should cover all glazed areas within the defined zone up to the edge of door daylight opening (FMVSS201) where it meets the roofline, B-pillar, C-pillar and door waistline. Seams in the airbag will not be penalized provided that the un-inflated area is no wider than 15mm. Any other areas where the airbag layers are connected will not be penalized provided that the surrounding areas are inflated and any un-inflated areas are no larger than 50mm in diameter or equivalent area or the sum of the major and minor axes of individual areas does not exceed 100mm. In the case that the un-inflated area would be larger than described above, the OEM shall provide data to demonstrate sufficient energy absorption is guaranteed.

Where a vehicle is fitted with a third row of foldable or removable seats, the third row (only) will be excluded from the assessment.

Incorrect Airbag Deployment

Any airbag(s) which does not deploy fully in the designed manner will attract a -1 point modifier applicable to each of the most relevant body part(s) for the affected occupant. For example, where a head curtain airbag is deemed to have deployed incorrectly, the penalty will be applied to the side impact driver's head (-1). Where the incorrect deployment affects multiple body parts, the modifier will be applied to each individual body part. For example, where a seat or door mounted side airbag fails to deploy correctly that is intended to provide protection to the head as well as the thorax, abdomen and pelvis, the penalty will be applied to all body regions, the head (-1), chest (-1), abdomen (-1) and pelvis (-1). The penalties are applicable to both the side and pole impacts, which are scaled down in the final vehicle rating.

The modifier will be applied even if the airbag was not intended to offer protection in that particular impact. For example, the penalty will be applied if a driver's knee airbag deploys incorrectly in a side or pole impact. In this case the modifier will be applied to both frontal impact driver knee, femur and pelvis body parts. Where a frontal protection airbag deploys incorrectly,

Door Opening during the Impact

When a door opens in the test, a minus one-point modifier will be applied to the score for that test. The modifier will be applied to the side impact assessment score for every door (including tailgates and moveable roofs) that opens. The number of door opening modifiers that can be applied to the vehicle score is not limited.

Door Opening Forces after the Impact

A check is made to ensure that the doors on the non-struck side can be opened. The doors on the

Scoring & Visualization

The protection provided for adults for each body region are presented visually, using colored segments within body outlines. The color used is based on the points awarded for that body region (rounded to three decimal places), as follows:

Green	'Good'	4.000 points
Yellow	'Adequate'	2.670 - 3.999 points
Orange	'Marginal'	1.330 - 2.669 points
Brown	'Weak'	0.001 - 1.329 points
Red	'Poor'	0.000 points

For the side barrier and pole impacts, all the individual regions are used. Results are shown separately for side barrier and pole impact.

The contribution of the side and pole impact tests to the Adult Occupant Protection Score is calculated by summing the body scores for the relevant body regions in each of the tests. The total score inside barrier and pole tests together is limited to 16 points. This is achieved by adding up the individual scores (after modifiers have been applied) for the side impact test (max. 16 points) and the pole test (max. 16 points) and dividing the result by two